Competing effects of particle and medium inertia on particle diffusion in viscoelastic materials, and their ramifications for passive microrheology

Tsutomu Indei,[1] Jay D. Schieber,[1,2] and Andrés Córdoba[1]

[1]*Department of Chemical and Biological Engineering and Center for Molecular Study of Condensed Soft Matter, Illinois Institute of Technology, 3440 South Dearborn Street, Chicago, Illinois 60616, USA*

[2]*Department of Physics, Illinois Institute of Technology, 3440 South Dearborn Street, Chicago, Illinois 60616, USA*

(Received 8 December 2011; published 20 April 2012)

We analyze the appropriate form for the generalized Stokes-Einstein relation (GSER) for viscoelastic solids and fluids when bead inertia and medium inertia are taken into account, which we call the inertial GSER. It was previously shown for Maxwell fluids that the Basset (or Boussinesq) force arising from medium inertia can act purely dissipatively at high frequencies, where elasticity of the medium is dominant. In order to elucidate the cause of this counterintuitive result, we consider Brownian motion in a purely elastic solid where ordinary Stokes-type dissipation is not possible. The fluctuation-dissipation theorem requires the presence of a dissipative mechanism for the particle to experience fluctuating Brownian forces in a purely elastic solid. We show that the mechanism for such dissipation arises from the radiation of elastic waves toward the system boundaries. The frictional force associated with this mechanism is the Basset force, and it exists only when medium inertia is taken into consideration in the analysis of such a system. We consider first a one-dimensional harmonic lattice where all terms in the generalized Langevin equation—i.e., the elastic term, the memory kernel, and Brownian forces—can be found analytically from projection-operator methods. We show that the dissipation is purely from radiation of elastic waves. A similar analysis is made on a particle in a continuum, three-dimensional purely elastic solid, where the memory kernel is determined from continuum mechanics. Again, dissipation arises only from radiation of elastic shear waves toward infinite boundaries when medium inertia is taken into account. If the medium is a viscoelastic solid, Stokes-type dissipation is possible in addition to radiational dissipation so that the wave decays at the penetration depth. Inertial motion of the bead couples with the elasticity of the viscoelastic material, resulting in a possible resonant oscillation of the mean-square displacement (MSD) of the bead. On the other hand, medium inertia (the Basset force) tends to attenuate the oscillations by the dissipation mechanism described above. Thus competition between bead inertia and medium inertia determines whether or not the MSD oscillates. We find that, if the medium density is larger than 4/7 of the bead density, the Basset damping will suppress oscillations in the MSD; this criterion is sufficient but not necessary to present oscillations.

DOI: 10.1103/PhysRevE.85.041504 PACS number(s): 83.10.Mj, 05.40.Jc

I. INTRODUCTION

Rheological properties of soft materials like polymer solutions, micellar solutions, polymer gels, etc. are usually characterized in mechanical ways; apply a dynamic deformation to the material and measure the resulting time- (or frequency-) dependent stress [1]. However, there are some critical limitations in these standard methods. First, the sample size must be so large as to fill fixtures of order 1 ml. Due to this limitation, small samples such as living cells cannot be measured [2]. Furthermore, the frequency window of the measurement is limited by fixture inertia and compliance (for example, $\omega < 10^2$–10^3 Hz for rotational rheometers). Because of this upper bound, there are limitations in characterizing fine structures and local dynamics of complex materials from a rheological point of view.

Microrheology, or microbead rheology, is a powerful alternative to measure viscoelastic properties of a soft material by tracking the motion of micrometer-sized tracer beads embedded in it [2–7]. In one-bead passive microrheology, a tracer bead of radius R ($\lesssim 1$ μm) is placed in the medium, and the mean-square displacement (MSD) $\langle \Delta r_{\rm b}^2(t)\rangle_{\rm eq} := \langle [\boldsymbol{r}_{\rm b}(t) - \boldsymbol{r}_{\rm b}(0)]^2\rangle_{\rm eq}$ of its position $\boldsymbol{r}_{\rm b}$ is followed by using some optical technique. The essence of one-bead passive microrheology for purely viscous (or Newtonian) fluids is as follows. The MSD of a bead in a purely viscous fluid is $\langle \Delta r_{\rm b}^2(t)\rangle_{\rm eq} = 6\mathcal{D}t$. The diffusion constant $\mathcal{D}$ is related with the friction coefficient ζ by the Einstein relation $\zeta = k_{\rm B}T/\mathcal{D}$, where $k_{\rm B}$ is the Boltzmann constant and T is the temperature. Assuming that fluid inertia is negligible, the Stokes law $\eta = \zeta/(6\pi R)$ holds between the viscosity η and the friction coefficient. Therefore, the MSD of the bead is related to the viscosity of the medium through the equation $\langle \Delta r_{\rm b}^2(t)\rangle_{\rm eq} = \frac{k_{\rm B}T}{\pi R\eta}t$ in the time domain, or, by taking the one-sided Fourier transform, $\langle \overline{\Delta r_{\rm b}^2}[\omega]\rangle_{\rm eq} = \frac{k_{\rm B}T}{\pi R(i\omega)^2\eta}$ in the frequency ω domain. The last equation is the classical Stokes-Einstein relation that allows us to estimate medium viscosity from the bead's MSD (and particle size).

For a viscoelastic medium, both the modulus and the friction of the fluid have time (or frequency) dependence due to the retardation effect of the host medium. Mason and Weitz proposed the generalized Stokes-Einstein relation (GSER) in 1995 [8] that relates the bead's MSD and the dynamic modulus $G^*(\omega)$ of the viscoelastic medium in the frequency domain. The GSER is obtained by simply replacing the Newtonian viscosity with the dynamic viscosity as $\eta \to G^*(\omega)/(i\omega)$ in the classical Stokes-Einstein relation, i.e.,

$$\left\langle \overline{\Delta r_{\rm b}^2}[\omega]\right\rangle_{\rm eq} = \frac{k_{\rm B}T}{\pi Ri\omega G^*(\omega)}. \tag{1}$$

Mason gave a derivation of Eq. (1) five years later [9], and we recently provided a detailed discussion on the derivation

of Eq. (1) [10]. In one-bead passive microrheology of viscoelastic fluids, analysis is typically made via the GSER (1). Microrheology can decrease the lower limit of the sample volume [2,11,12] and increase the upper limit on frequency of conventional mechanical rheology. The GSER is comprised of two important relations as in the classical relation; one is the Einstein part that associates the bead's MSD with the frequency-dependent friction [or memory kernel (function)], and the other is the Stokes part that connects the memory function and the dynamic modulus of the medium. The memory function does not appear explicitly in Eq. (1) [8]; it connects two relations only implicitly.

Neither medium inertia nor bead inertia is taken into consideration in the derivation of Eq. (1). In our recent publication [10], we derived and justified the GSER for viscoelastic fluids that includes inertial effects of both the bead and the medium. We studied the Maxwell fluid and its extension to show the following. The MSD of the bead in the Maxwell fluid does not satisfy the proper initial condition $\langle r_{\rm b}^2(t)\rangle_{\rm eq} = 0$ when inertial effects of the bead are not considered. If bead inertia is included properly, the ballistic motion of the bead is recovered and the proper initial condition is satisfied as expected. However, the MSD oscillates at all $t \lesssim \lambda$ (λ is the relaxation time of the Maxwell medium), indicating that not only the early-time behavior of the ballistic motion, but also the viscoelastic behavior whose time scale is much longer than the ballistic time scale, is affected considerably. This oscillatory MSD is very different from the results of the original inertialess GSER and also experimental observations. Also, the nonoscillatory MSD from the inertialess GSER is never recovered by taking the zero-mass limit of the bead [13]. On the contrary, the frequency of the oscillation diverges in this limit. Thus the inertialess limit of the bead is singular. We found that if a purely viscous component is added to the Maxwell fluid (or, in other words, if a δ function is added to the memory kernel), the oscillation in the MSD is attenuated in the zero-mass limit of the bead because of energy dissipation of the bead by the purely viscous component. Importantly, the attenuation is achieved no matter how small the viscosity from the purely viscous component is. For an infinitesimal viscosity, the MSD from the inertialess GSER is achieved at $t > 0$. Even in the absence of the purely viscous component, the inertial oscillation of the MSD can be attenuated inside the typical experimental time window if there are other relaxation modes outside the frequency window of the dynamic modulus in which the Maxwell behavior is observed.

For a single-mode Maxwell fluid, elasticity of the medium is dominant and viscosity is suppressed in the high-frequency regime $\omega \gg 1/\lambda$, and therefore the medium does not allow the embedded bead to dissipate its mechanical energy into the medium by an ordinary Stokes-type dissipation in this frequency regime. The bead cannot fluctuate in the absence of the dissipation as a result of the fluctuation-dissipation theorem [14], and the lack of fluctuations indicates a breakdown of the GSER as well as of passive microrheology. This observation is intuitively plausible but obviously unsatisfactory. We indicated in Ref. [10] that this complaint is resolved by taking account of medium inertia. Medium inertia plays the same role as the purely viscous element in the high-frequency regime $\omega \gg 1/\lambda$ where the dynamic modulus becomes a real constant (giving a plateau). That is, the so-called Basset (or Boussinesq) force arising from medium inertia plays the same role as a frictional force. Consequently the bead can experience Brownian motion associated with this dissipation mechanism. Also, the MSD's oscillation is attenuated by the Basset force's frictional nature. In fact, the oscillation never occurs if the medium density and bead density are comparable. Thus bead inertia and medium inertia compete for the generation of the oscillation in the MSD.

One of the objectives of the present paper is to reveal the mechanism of energy dissipation caused by the Basset force due to medium inertia. To this end, we consider purely elastic solids without viscosity to make the problem clear. We show that, in the presence of medium inertia, elastic shear waves excited by the bead's vibration transmit the mechanical energy of the bead toward the boundaries of the medium. If the boundary is infinitely far from the bead position, reflections of the wave from the boundary are nonexistent. This causes the energy dissipation of the bead even in purely elastic solids, indicating that GSER works if inertial effects are included. In a real system, of course, the boundaries are a finite distance away from the bead position, but in reality there also exists Stokes-type dissipation from some finite amount of viscosity of the medium that may attenuate such waves before they reach the medium boundary. Basset damping for a purely elastic medium was also suggested in Ref. [15].

We also study viscoelastic solids and derive the formula that relates the bead's MSD and G^* of the medium when both bead and medium inertia are taken into account. We call this formula the inertial GSER (IGSER). We derive both the Einstein part and the Stokes part of the IGSER for viscoelastic solids. The result is the same as that for viscoelastic fluids provided in our recent paper [10] where we did not yet use the abbreviation IGSER. The medium is assumed to be incompressible throughout this article. Finally, we study a competition between bead inertia and medium inertia that determines whether or not the MSD oscillates. We show in general that, if the medium density is larger than $4/7$ of the bead density, the Basset damping will suppress oscillations in the MSD; this criterion is sufficient but not necessary to suppress oscillations. The results are independent of details of the relaxation spectrum of the medium. We were less specific about this condition in our recent paper [10].

This paper is organized as follows. We start by studying the simplest physical model of a purely elastic solid, a harmonic regular lattice, in the following section. This particular system contains sufficient physics of a purely elastic solid to illustrate all points stated above, i.e., energy dissipation of the tagged bead by means of the radiation of elastic waves, effective friction of the lattice associated with this radiational dissipation, and an interpretation of the Basset force. In Sec. III, we provide the generalized Langevin equation (GLE) of the tracer bead and derive the Einstein part of the IGSER for general viscoelastic solids (not restricted to lattice systems) that takes account of bead inertia. In Sec. IV, the Stokes component of the IGSER for viscoelastic solids that includes inertial effects of the medium is derived. The IGSER for solids (and fluids) is given explicitly in Sec. V for two expressions; one expresses the MSD in terms of a given G^*, and the other inversely expresses G^* from the MSD. In Sec. VI, the implication of the Basset force in terms of the energy radiation by shear waves is

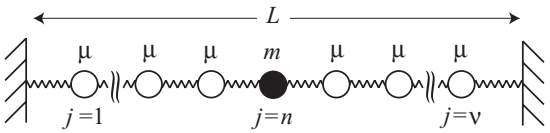

FIG. 1. Sketch of the one-dimensional harmonic lattice formed by ν beads. The tagged bead is the nth one located near the center.

discussed. In Sec. VII, we study the competing effects of bead inertia and medium inertia for MSD oscillation, and derive the sufficient conditions for the oscillation not to occur. In Sec. VIII, a relation for the dynamics of a bead embedded in viscoelastic solids and that trapped by an external force in viscoelastic fluids is discussed. Conclusions are made in Sec. IX.

II. ONE-DIMENSIONAL LATTICE MODEL OF ELASTIC SOLIDS

In this section, we consider a one-dimensional harmonic lattice and a tagged bead embedded in it (see Fig. 1). This system is the simplest model of purely elastic solids in which a small bead is embedded, but probably the best example to figure out (i) the tagged bead's energy dissipation along with the radiation of elastic waves excited by the tagged bead's vibration, (ii) the Brownian motion of the tagged bead associated with this radiational dissipation by the fluctuation-dissipation theorem (FDT), (iii) the implication of the Basset force of the medium, and (iv) the separation of the purely elastic element from the memory function while keeping this element in the Basset force. All these properties also hold true for three-dimensional continuum elastic solids as shown in the following sections. Here we consider the lattice because the equation of motion of the tagged bead can be transformed into the expression of the generalized Langevin equation in a rigorous manner by projection-operator methods [16], and therefore we can concretely see the behavior of, for example, the memory function that reflects the tagged bead's characteristic motion in the medium, giving us insight into the tracer bead's motion in more realistic systems.

The derivations of the GLE for harmonic lattices were accomplished several decades ago by Deutch and Silbey [17] and later by Wada and Hori [18], both for a one-dimensional lattice in the displacement space for the projection procedure, and by Wada [19] for arbitrary dimension and several lattice structures in the phase space of displacement and momentum for the projection. However, observations (i)–(iv) above have not been pointed out so far, to our knowledge. First, we briefly review these relatively old results in Sec. II A. Detailed calculations can be found in Appendix B and in Refs. [17–19]. Next, in Sec. II B, we give these results interpretations in terms of (i)–(iv) to understand correctly the microrheology of purely elastic solids and implicitly of viscoelastic materials.

A. GLE of a tagged bead in a lattice

We consider a one-dimensional lattice composed of ν beads aligned on the r axis. Neighboring beads are connected by a harmonic potential with a spring constant H_s, and all beads are allowed to move one-dimensionally only along the r axis without excluded volume interaction among beads (or between beads and walls). See Fig. 1. Both ends of the lattice are fixed and separated from each other by a distance L. The rest length of a bond is then $h := L/(\nu+1)$. Of ν beads, we regard the nth one as the tagged bead. Other beads on the lattice represent elements of the medium. The tagged bead has a mass m but all the other beads have a different mass μ, in general. Thus, the one-dimensional medium density is $\rho = (\nu-1)\mu/L$. We assume that the tagged bead is located near the center of the lattice ($n \simeq \nu/2$) without loss of generality. The jth bead has momentum p_j and displacement $\delta r_j := r_j - \bar{r}_j$ from its rest position $\bar{r}_j := jh$. Thus the system is characterized by a 2ν-dimensional vector in the phase space of momentum and displacement of all beads $\boldsymbol{X} = (\boldsymbol{p},\delta\boldsymbol{r})$, where $\boldsymbol{p} := (p_1,\ldots,p_\nu)$ and $\delta\boldsymbol{r} := (\delta r_1,\ldots,\delta r_\nu)$.

We are interested in the situation that the tagged bead is a macroscopic object while the surrounding beads are microscopic elements comprising the medium. In other words, variables $\boldsymbol{X}_j := (p_j,\delta r_j)$ with respect to beads other than the tagged one ($j \neq n$) are microscopic fast variables, whereas $\boldsymbol{X}_n = (p_n,\delta r_n)$ for the tagged bead are macroscopic slow variables. The dynamics of the tagged bead can be decomposed into the part which is directly relevant to the tagged bead and the remaining part that reflects the dynamics of other beads. This decomposition can be done by applying the projection-operator technique (see, for example, Ref. [14]). We first solve the equation of motion for the total system [given by Eq. (B2) in Appendix B]. Then, by substituting the result into the projection-operator results for the tagged bead in phase space, the equation of motion for the tagged bead [given by Eq. (B4)] is transformed into the form of a GLE as

$$\frac{dp_n(t)}{dt} = -\frac{k_BT}{\langle\delta r_n^2\rangle_{\rm eq}}\delta r_n(t) - \int_0^t \frac{\zeta(t-t')}{m}p_n(t')dt' + f_B(t),$$
$$p_n(t) = \frac{d\delta r_n(t)}{dt}. \tag{2}$$

See Appendix B for details. The last equations are closed with respect to the tagged bead's displacement $\delta r_n(t)$. Information about the medium (or the other beads) is included in the memory function $\zeta(t)$ with respect to the "frictional force" and in the last term $f_B(t)$ as the "random force" on the tagged bead. These two forces come from the term $d\boldsymbol{X}_n(t)/dt$ of Eq. (B4) projected onto the space orthogonal to the tagged bead's space $\boldsymbol{X}_n$, and represent the dynamics of the tagged bead associated with the other beads' fast motion. So far, $f_B(t)$ is not really a stochastic force and the memory integral is not a dissipative force in a literal sense because contraction of information on the other beads has not yet been made in the derivation of Eq. (2) from the deterministic equation (B2) for a finite system. The quotation marks around the terms indicate these facts. For simplicity we neglect these quotation marks in the following. The Brownian random force is obtained in an exact form as

$$f_B(t) = H_s[\boldsymbol{A}\cdot\delta\tilde{\boldsymbol{r}}(t)]_n, \tag{3}$$

where $\boldsymbol{A}$ is the Rouse matrix (see Appendix B) and $\delta\tilde{\boldsymbol{r}}(t)$ is given by Eq. (B22). The memory function is also rigorously derived as

$$\zeta(t) = H_s[\cos(\sqrt{\boldsymbol{A}_0}\omega_\mu t/2)\cdot\boldsymbol{A}]_{nn}. \tag{4}$$

A subscript n (or nn) indicates taking the nth [or (n,n)th] element of the vector (matrix). The modified Rouse matrix $\boldsymbol{A}_0$ takes 0 for all elements of the nth column but other elements are the same as in $\boldsymbol{A}$, and

$$\omega_\mu := 2\sqrt{\frac{H_s}{\mu}}. \tag{5}$$

The cosine of a matrix is defined by the Taylor series. Equations (3) and (4) are related via the fluctuation-dissipation theorem of the second kind,

$$\langle f_B(t) f_B(0)\rangle_{eq} = k_B T \zeta(t). \tag{6}$$

The angular brackets $\langle\cdots\rangle_{eq}$ in Eqs. (2) and (6) represent canonical averaging with respect to the initial distribution [see Eq. (A4) in Appendix A].

The first term in the right-hand-side of the GLE (2) is the part of $d\boldsymbol{X}_n(t)/dt$ projected onto the space $\boldsymbol{X}_n$ associated with the tagged bead, and therefore depends only on the tagged bead's displacement at the present time t. We refer to this term as the *elastic term* in the following. The proportionality coefficient of the elastic term is $k_B T/\langle \delta r_n^2\rangle_{eq} = H_s/C_{nn}$ where $C_{nn} = n(\nu+1-n)/(\nu+1)$ is the (n,n) element of the Kramers matrix $\boldsymbol{C} = \boldsymbol{A}^{-1}$ [20]. This coefficient $k_B T/\langle \delta r_n^2\rangle_{eq}$ is called the frequency matrix [16] (although it is not actually a matrix in this case). Since the tagged bead is located near the center of the lattice, the coefficient of the elastic term is $H_s/C_{nn} \sim 4H_s/\nu$.

B. Dissipation of the tagged bead and Basset force of the lattice

The memory function $\zeta(t)$ given by Eq. (4) reveals two types of periodic behavior as shown in Fig. 2. One is the damped oscillation with period $\tau := 2/\omega_\mu = h/C$ where $C = h\omega_\mu/2 = h/\tau$ is the sound velocity of the lattice. This damped oscillation is ascribed to the microscopic motion of the lattice, or, in other words, local correlation of the tagged bead and neighboring beads. The other periodic behavior does not decay and has the longer period $\mathrm{T} := L/C = 2\nu/\omega_\mu$. This periodicity originates from the correlation of the tagged bead's motion and the reflected elastic wave which was originally excited and radiated by the tagged bead's vibration and reflected at the boundaries. Thus the correlation attenuates temporally locally within a time window $0 \leqslant t < \mathrm{T}$ but does not decay in the long run because of the reflected wave at the boundaries.

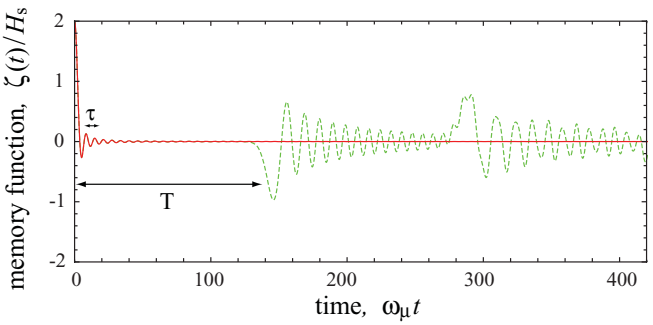

FIG. 2. (Color online) The memory function for the one-dimensional harmonic lattice as a function of time. The total number of beads is $\nu = 71$. Dotted line, $\zeta(t) = H_s[\cos(\sqrt{\boldsymbol{A}_0}\omega_\mu t/2)\cdot\boldsymbol{A}]_{nn}$; solid line, $\zeta(t) = \zeta_0 J_1(\omega_\mu t)/t$. The two lines are overlapping at $0 \leqslant t \lesssim T$.

1. Thermodynamic limit

Now we take the thermodynamic limit $\nu\to\infty, L\to\infty$ while keeping the rest length h constant. The period of the memory function $\mathrm{T} = 2\nu/\omega_\mu$ goes to infinity, thereby eliminating the effects of the reflection of waves at boundaries by this limit. On the other hand, the microscopic time scale $\tau = 2/\omega_\mu$ does not change. Equation (4) reduces to

$$\zeta(t) = \zeta_0 \frac{J_1(\omega_\mu t)}{t}, \tag{7}$$

or, in the frequency domain,

$$\bar{\zeta}[\omega] = \zeta_0[\sqrt{1-(\omega/\omega_\mu)^2} - i\omega/\omega_\mu], \tag{8}$$

where $\zeta_0 := 2\sqrt{H_s\mu}$ is a friction constant and J_1 is the Bessel function of the first kind. See the solid line in Fig. 2. The memory function given by Eq. (7) goes to 0 in the long-time limit. Thus the mechanical energy of the tagged bead dissipates in the sense that it travels infinitely far from the bead position along with the wave and never returns. This (already known) consequence is important for correctly understanding the diffusion of the tagged bead and its ramification for microrheology of purely elastic solids. Even if the viscous component does not exist in the medium, the tagged bead can dissipate its energy by radiation toward the infinite boundary [observation (i)]. Equation (7) describes the friction arising from this radiational dissipation. The tagged bead experiences Brownian motion due to radiational dissipation, *rather than* the ordinary Stokes-type dissipation, via the FDT [observation (ii)]. Thus the IGSER works even for purely elastic solids where the Stokes-type dissipation is not allowed. These facts also hold in a three-dimensional continuum medium as shown in Sec. VI.

The elastic term diminishes in the thermodynamic limit as a result of the low dimensionality of the system. For three-dimensional lattice systems, the elastic term remains [19].

There is a memory in the tagged-bead motion because the microscopic correlation time τ among beads is still finite, so that the bead's motion is not (yet) a Markovian process.

2. Markovian limit and continuum limit

By taking the limit $\omega_\mu/\omega\to\infty$ for any given ω (or $\tau/t\to 0$ for any t) while keeping the coefficient of the momentum $\zeta_0/m = (\mu/m)\omega_\mu$ in the memory integral of Eq. (2) constant (μ/m goes to 0), the dynamics of the tagged bead becomes a Markovian process. That is, $\bar{\zeta}[\omega]$ [Eq. (8)] approaches $\zeta_0 = 2\sqrt{H_s\mu}$, and therefore $\zeta(t)$ becomes proportional to ζ_0 and the delta function $\delta(t)$.

The friction constant $\zeta_0 = 2\sqrt{H_s\mu}$ is associated with the energy dissipation of the tagged bead by radiation of the elastic wave emitted by the tagged bead's vibration. This fact is directly confirmed by calculating the rate of energy transfer [21] of the bead. To this end, it is convenient to take the continuum limit of the lattice. The equation (B2) of motion of the lattice, except for $j = n$ (i.e., the tagged bead's

displacement), is explicitly written as $\mu\frac{d^2\delta r_j}{dt^2} = H_s(\delta r_{j+1} - 2\delta r_j + \delta r_{j-1})$. Dividing this equation by h and taking the limit $h \to 0$ while keeping $\rho = \mu/h$ and the modulus $G := hH_s$ constant (or keeping ρ and the sound velocity $C = h\omega_\mu/2 = \sqrt{G/\rho}$ constant), this equation becomes the wave equation for the displacement field of a string,

$$\rho\frac{\partial^2 u(r,t)}{\partial t^2} = G\frac{\partial^2 u(r,t)}{\partial r^2}, \tag{9}$$

where the displacement field $u(r,t)$ at position r on the string corresponds to the jth bead's displacement $\delta r_j(t)$ on the lattice. This continuum limit $h \to 0$, while ρ and C are kept constant, also gives the Markovian limit $\omega_\mu \to \infty$ and $\mu \to 0$ stated above, so that the tagged bead's dynamics becomes Markovian in this limit.

To mimic the tagged bead's harmonic oscillation at the origin, we consider the forced harmonic vibration of the string with frequency ω at the origin, i.e., $u(r = 0,t) = \epsilon e^{i\omega t}$, where $\epsilon > 0$ is the amplitude of the oscillation. The solution of Eq. (9) that satisfies this boundary condition and the outward radiation condition from the origin is just $u(r,t) = \epsilon e^{i(\omega t + k|r|)}$, where the wave number is $k := -\omega/C = -\omega\sqrt{\rho/G}$. Then the rate of energy transfer $P(r_0)$ past a point $r = r_0$ is

$$P(r_0) = -G\frac{\partial u(r,t)}{\partial r}\dot{u}(r,t)\bigg|_{r=r_0} \tag{10}$$

$$= \sqrt{\rho G}\dot{u}(0,t - r_0/C)^2. \tag{11}$$

The rate of energy transfer $P(-r_0)$ past a point $r = -r_0$ takes the same value as $P(r_0)$ due to the symmetry. Therefore the energy that leaves the domain of the string $-r_0 \leqslant r \leqslant r_0$ per unit time is $P_{\text{total}}(r_0) = 2P(r_0) = 2\sqrt{\rho G}\dot{u}(0,t - r_0/C)^2$, and this corresponds to the rate of energy loss $\zeta_0\dot{u}(0,t)^2$ of the tagged bead supposed to be located around the origin. The time lags by r_0/C due to the delay of the wave propagation. Thus the friction constant of the tagged bead is $\zeta_0 = 2\sqrt{\rho G} = 2\sqrt{\mu H_s}$, corresponding to the one derived above.

Note that ζ_0 contains the medium density. This fact indicates that the frictional force on the tagged bead derived here, which comes from the radiational energy dissipation, is ascribed to medium inertia. This form of ζ_0, i.e., $\sqrt{\rho G}$, is the scaling that typically appears in the so-called Basset force from medium inertia on the sphere embedded in the medium as discussed in Sec. IV. Thus we can know for the one-dimensional solid that the frictional force associated with the radiational energy dissipation of the tagged bead toward the infinite boundary of the system is the Basset force [observation (iii)]. Actually, this fact holds true in general for three-dimensional continuum elastic solids (see Sec. VI). The Basset force is derived in Sec. IV for a viscoelastic medium.

Finally, it should be noted that the elastic term is separated from the memory function in the GLE (2) as a natural consequence of the projection-operator methods [observation (iv)]. The same goes for general elastic solids as shown in Sec. III A. Due to the separation, the memory function does not include the contribution from a purely elastic element represented by the elastic term. This fact assures that the memory function decays properly in the long-time limit, so does the autocorrelation of the random force due to the FDT. On the other hand, the contribution from a purely elastic element remains in the Basset force. This is because the Basset force of solids comes from the elasticity of the medium as shown above.

III. EINSTEIN COMPONENT FOR VISCOELASTIC SOLIDS (THREE DIMENSIONS)

A. GLE for viscoelastic solids

The Einstein component of IGSER is obtained by solving the GLE of a tracer bead embedded in a three-dimensional (3D) viscoelastic solid. The GLE for solids can be derived by applying the projection-operator method (see Appendix C) as in the case of lattice systems. The derivation of the GLE requires a special time $t = 0$ at which the initial conditions of dynamical variables are specified. The lower limit of the memory integral of Eq. (2) originates from this initial time. However, as discussed by Kubo *et al.* [14], pp. 37–39], it is desirable to modify the GLE to the explicitly stationary GLE with the lower integral limit $-\infty$. The GLE thus obtained is

$$m\frac{d^2\delta\boldsymbol{r}_b(t)}{dt^2} = -\boldsymbol{H}_e\cdot\delta\boldsymbol{r}_b(t) - \int_{-\infty}^{t}\zeta(t-t')\frac{d\delta\boldsymbol{r}_b(t')}{dt'}dt' + \boldsymbol{f}_B(t). \tag{12}$$

The bead motion described by Eq. (12) does not depend on the initial condition at any finite time thanks to the lower integral limit $-\infty$. The medium is assumed to be isotropic. $\delta\boldsymbol{r}_b(t) := \boldsymbol{r}_b(t) - \overline{\boldsymbol{r}}_b$ is the deviation of the tracer bead from its mean position $\overline{\boldsymbol{r}}_b$ and m is the tracer's mass. The mean-square displacement of the deviation $\langle\Delta\delta r_b^2(t)\rangle_{eq} := \langle[\delta\boldsymbol{r}_b(t) - \delta\boldsymbol{r}_b(0)]^2\rangle_{eq}$ in the long-time limit is twice the second moment of the bead's deviation in equilibrium, i.e., $\langle\Delta\delta r_b^2(\infty)\rangle_{eq} = \langle\delta r_b^2(\infty)\rangle_{eq} + \langle\delta r_b^2(0)\rangle_{eq} = 2\langle\delta r_b^2\rangle_{eq}$ since the autocorrelation of the deviation decays.

The elastic term $-\boldsymbol{H}_e\cdot\delta\boldsymbol{r}_b(t)$ in GLE (12) describes the cooperative motion of the bead and assures that the bead motion is restricted to the region around its most stable position due to the constraint by the surrounding medium. The coefficient matrix $\boldsymbol{H}_e$ is the so-called frequency matrix [16], which is proportional to the identity matrix $\boldsymbol{\delta}$ in an isotropic medium, i.e., $\boldsymbol{H}_e = H_e\boldsymbol{\delta}$, where the magnitude is given by

$$H_e = \frac{3k_BT}{\langle\delta r_b^2\rangle_{eq}} = \frac{6k_BT}{\langle\Delta\delta r_b^2(\infty)\rangle_{eq}}. \tag{13}$$

For viscoelastic fluids, the bead diffuses away as time passes so that $\langle\delta r_b^2\rangle_{eq} = \infty$, and therefore there is no elastic term in the GLE for a bead embedded in fluids.

Note that the contribution from the pure elasticity of the medium represented by the elastic term is separated from the memory function. This guarantees that the memory function decays in the long-time limit. Otherwise an unphysical constant would remain in the autocorrelation of the random force, which is not appropriate.

B. Derivation of the Einstein component of the IGSER

The MSD of the bead in a viscoelastic solid is derived as a functional of the memory function by solving the GLE (12). This relation is the Einstein component of the IGSER. The Einstein component for solids has almost the same form as that

for fluids. The only difference is that there exists a frequency matrix $\boldsymbol{H}_\mathrm{e}$ for solids outside of the memory function. Here we show an outline of the derivation of the Einstein component for isotropic viscoelastic solids. The detailed calculation for fluids is provided in our recent paper [10], giving the same results derived by Mason [9].

Taking the two-sided Fourier transform of both sides of Eq. (12), we obtain

$$\delta \boldsymbol{r}_\mathrm{b}[\omega] = \alpha(\omega)\boldsymbol{f}_\mathrm{B}[\omega], \tag{14}$$

where

$$\alpha(\omega) := \frac{1}{H_\mathrm{e} + i\omega\bar{\zeta}[\omega] - m\omega^2} \tag{15}$$

is the frequency-dependent complex compliance. We indicate the two-sided Fourier transform $\int_{-\infty}^{\infty} e^{-i\omega t}\cdots dt$ by a frequency argument with square brackets, and a one-sided Fourier transform is indicated by an overbar with square brackets such as $\bar{\zeta}[\omega]$. The desired equation for solids can be obtained by replacing $\bar{\zeta}[\omega]$ with $H_\mathrm{e}/(i\omega) + \bar{\zeta}[\omega]$ in the Einstein component for fluids including bead inertia [10], i.e.,

$$\left\langle \overline{\Delta\delta r_\mathrm{b}^2}[\omega]\right\rangle_\mathrm{eq} = \frac{6k_\mathrm{B}T}{i\omega(H_\mathrm{e} + i\omega\bar{\zeta}[\omega] - m\omega^2)}. \tag{16}$$

The power spectral density (PSD) $I(\omega)$ of the fluctuating bead motion is also given by this replacement, i.e.,

$$\begin{aligned} I(\omega) &= -\mathrm{Re}\left\{\frac{6k_\mathrm{B}T}{i\omega(H_\mathrm{e} + i\omega\bar{\zeta}[\omega] - m\omega^2)}\right\} \\ &= 6k_\mathrm{B}T\frac{|\mathrm{Im}\{\alpha(\omega)\}|}{\omega}, \end{aligned} \tag{17}$$

where $\mathrm{Re}\{\cdots\}$ and $\mathrm{Im}\{\cdots\}$ indicate taking the real and imaginary parts of the argument, respectively. The last equation is the fluctuation-dissipation relation (or theorem) [22].

C. Effects of the purely elastic component on inertial oscillation of the MSD

It has been shown that inertial motion of the bead couples with the elasticity of the medium, resulting in the resonant oscillation of the MSD of the bead [10,13,23,24]. If there is a purely viscous element in the medium, it tends to attenuate the oscillation since the purely viscous element dissipates the kinetic energy of the bead [10,24]. A broad relaxation spectrum can also damp the oscillation inside an experimental time window [10,13]. In solids, the oscillations can be enhanced due to the presence of the purely elastic component of the medium. Here we show how pure elasticity affects the MSD oscillation (i.e., inertial effects of the bead) for viscoelastic solids. The effects of medium inertia or Basset force are discussed in Secs. IV and VII.

We consider a four-parameter model comprised of a purely elastic element [with elasticity $g_\mathrm{e} = H_\mathrm{e}/(6\pi R)$], a single-mode Maxwell element (with plateau modulus g and relaxation time λ), and a purely viscous element (with viscosity η_0). The dynamic modulus of this solid is

$$G^*(\omega) = g_\mathrm{e} + g\frac{i\omega\lambda}{1 + i\omega\lambda} + i\omega\eta_0. \tag{18}$$

The purely elastic component suggests a permanent network in the medium while the purely viscous element suggests a solvent. Other viscoelastic properties are represented by a single Maxwell element alone. The memory function is the one from which the pure elasticity is subtracted because the pure elasticity already exists outside the memory function (see Sec. IV A), i.e.,

$$\bar{\zeta}[\omega] = \frac{6\pi R[G^*(\omega) - g_\mathrm{e}]}{i\omega} = \frac{\lambda H}{1 + i\omega\lambda} + \zeta_0, \tag{19}$$

where we have defined $H := 6\pi Rg$ and $\zeta_0 := 6\pi R\eta_0$. Substituting Eq. (19) into Eq. (16), we obtain the MSD in the frequency domain as

$$\left\langle \overline{\Delta\delta r_\mathrm{b}^2}[\omega]\right\rangle_\mathrm{eq} = \frac{6k_\mathrm{B}T}{i\omega}\frac{1 + i\omega\lambda}{\lambda m(i\omega)^3 + (m + \lambda\zeta_0)(i\omega)^2 + (\lambda H_\mathrm{e} + \lambda H + \zeta_0)i\omega + H_\mathrm{e}}, \tag{20}$$

and the corresponding PSD as

$$\begin{aligned} I(\omega) &= -\mathrm{Re}\left\{\left\langle \overline{\Delta\delta r_\mathrm{b}^2}[\omega]\right\rangle_\mathrm{eq}\right\} \\ &= \frac{6k_\mathrm{B}T(\zeta_0\lambda^2\omega^2 + \zeta_0 + \lambda H)}{(\lambda m)^2\omega^6 + [m^2 - 2m\lambda^2(H_\mathrm{e} + H) + (\lambda\zeta_0)^2]\omega^4 + \left[\lambda^2(H_\mathrm{e} + H)^2 + 2\lambda H\zeta_0 + \zeta_0^2 - 2mH_\mathrm{e}\right]\omega^2 + H_\mathrm{e}^2}. \end{aligned} \tag{21}$$

The zero points of the polynomial in the denominator of Eq. (20) determine the characteristic frequencies (or times) of the bead autocorrelation. The order of the polynomial (or the number of characteristic times) is the number of relaxation modes N plus one from the bead's inertial motion. For the present model, $N = 2$ so that there are three relaxation times in total. If the MSD does not oscillate, these times are the ballistic time λ_b related to the bead inertia, the first elastic relaxation time τ_e above which the first elastic plateau appears in the MSD, and the second elastic relaxation time τ_e' for the second plateau in the longer-time regime. These times are approximately given by

$$\tau_{\mathrm{b,e}} \simeq \frac{2m\lambda}{m + \lambda\zeta_0 \pm \sqrt{(m + \lambda\zeta_0)^2 - 4m\lambda(\lambda H_\mathrm{e} + \lambda H + \zeta_0)}}, \tag{22}$$

$$\tau_\mathrm{e}' \simeq \frac{2(m + \lambda\zeta_0)}{\lambda H_\mathrm{e} + \lambda H + \zeta_0 - \sqrt{(\lambda H_\mathrm{e} + \lambda H + \zeta_0)^2 - 4H_\mathrm{e}(m + \lambda\zeta_0)^2}}, \tag{23}$$

$$\lambda_\mathrm{b} := \sqrt{\tau_\mathrm{b}\tau_\mathrm{e}}, \tag{24}$$

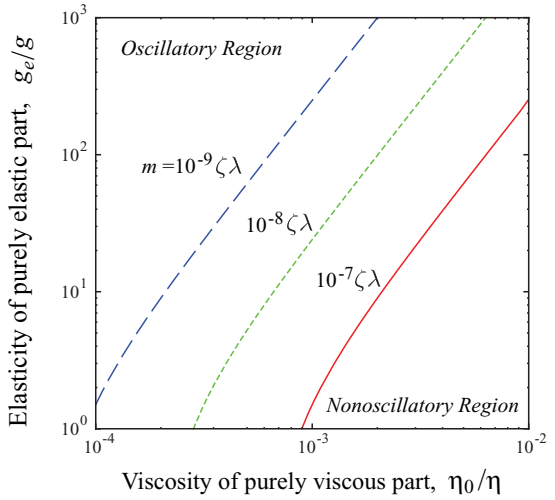

FIG. 3. (Color online) Phase diagram of the bead oscillation for the four-parameter model of a viscoelastic solid [Eq. (18)]. The medium inertia is not considered. The bead mass is different for each curve. A set of viscoelastic parameters in the region above each curve leads to the oscillation of the MSD. $\zeta := \lambda H$ is the friction of the Maxwell element and horizontal axis is scaled by $\eta := \zeta/(6\pi R)$. Vertical axis is scaled by $g = H/(6\pi R)$.

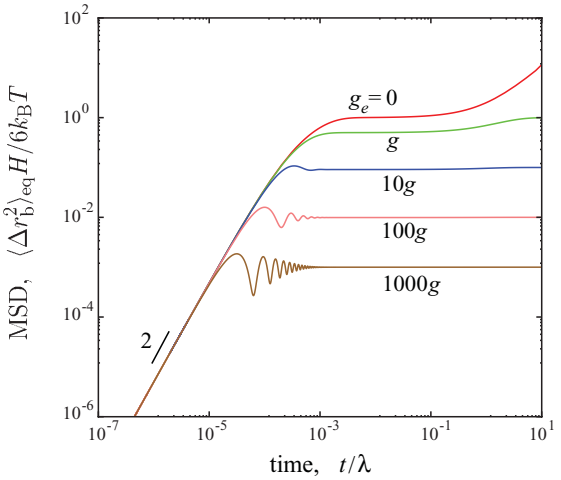

FIG. 4. (Color online) Mean-square displacement of a bead with the mass $m = 10^{-7}\zeta\lambda$ embedded in a four-parameter model of a viscoelastic solid. Medium inertia is not considered. The elasticity $g_e = H_e/(6\pi R)$ of the purely elastic component is increasing from top to bottom for a fixed elasticity $g = H/(6\pi R)$ of the Maxwell element of the medium. ζ_0 is set to $10^{-3}\zeta$.

where τ_b (τ_e) takes the positive (negative) sign in Eq. (22). Derivation of $\tau_{b,e}, \tau_e'$, and the expression for the MSD are given in Appendix D. The argument of the square root in the denominator of τ_e' is usually positive because the viscosity of the solvent ζ_0 is typically much smaller than that of the viscoelastic component, $\zeta = \lambda H$, and the bead mass is small, $m \ll \lambda^2 H = \zeta\lambda$. On the other hand, the argument of the square root of $\tau_{b,e}$ can be negative if the inequality condition

$$H_e + H > \frac{(\lambda\zeta_0 - m)^2}{4m\lambda^2} \tag{25}$$

is satisfied. This condition (25) makes $\tau_{b,e}$ complex quantities, thereby causing an oscillation in the MSD with frequency

$$\omega_m := \frac{\sqrt{4m\lambda(\lambda H_e + \lambda H + \zeta_0) - (m + \lambda\zeta_0)^2}}{2m\lambda}. \tag{26}$$

See Fig. 3. The oscillation decays at $t \gtrsim \lambda_e := 2/(1/\tau_b + 1/\tau_e) = \frac{2m\lambda}{m+\lambda\zeta_0}$ because of the energy dissipation caused by viscous components. These times $1/\omega_m$ and λ_e (and τ_e') are the time constants when inequality (25) is fulfilled.

Condition (25) indicates that the oscillation tends to occur more easily for solids than for fluids due to the presence of a purely elastic component (see Fig. 4). Also, with increasing elasticity (g and g_e), the period of the oscillation $1/\omega_m$ becomes smaller while the terminal λ_e of the oscillation remains constant. Therefore, the amplitude of the oscillation becomes larger.

The results shown here originate from the inertial effects of the bead alone; medium inertia is not taken into account. The combined effects of bead inertia and medium inertia are discussed in Sec. VII. (Interestingly, if medium inertia is considered, the elasticity of the purely elastic element does not affect the sufficient condition of the oscillation.)

IV. STOKES COMPONENT FOR VISCOELASTIC SOLIDS

A. Derivation of the Stokes component of the IGSER

The Stokes component relates the medium viscoelasticity and the memory function (or the complex compliance). Below we derive the Stokes component of the IGSER for viscoelastic solids by applying the results for Newtonian and viscoelastic fluids [25,26]. We consider isotropic incompressible solids. The radius R of the bead embedded in the medium is assumed to be much larger than the microscopic structure of the medium (such as the mesh size of a polymer network) so that the medium is treated as a continuum.

With the help of results for Newtonian fluids [26], the radial component u_r and the polar component u_θ of the displacement field of the viscoelastic solids in the presence of a vibrating spherical bead are respectively obtained in the frequency domain as $u_r[\omega] = -[a(\omega)e^{ik(\omega)r}(\frac{2}{r^2} - \frac{2}{ik(\omega)r^3}) + \frac{2b(\omega)}{r^3}]\cos\theta$ and $u_\theta[\omega] = [a(\omega)e^{ik(\omega)r}(\frac{ik(\omega)}{r} - \frac{1}{r^2} + \frac{1}{ik(\omega)r^3}) - \frac{b(\omega)}{r^3}]\sin\theta$, where $a(\omega) := -\frac{3R}{2ik(\omega)}e^{-ik(\omega)R}u_0[\omega]$ and $b(\omega) := \frac{R[3-3ik(\omega)R-k(\omega)^2R^2]}{2k(\omega)^2}u_0[\omega]$ are r-independent constants determined by the boundary conditions, and $k(\omega) := -\omega/C(\omega)$ is the frequency-dependent complex wave number [$C(\omega) = \sqrt{G^*(\omega)/\rho}$ is the frequency-dependent complex transverse sound velocity]. The sign of $k(\omega)$ was chosen so that the outward radiation condition and the decaying condition at infinity of the displacement field (or shear waves) are attained. See Appendix E for details of the derivation.

The relevant components of the stress tensor in the frequency domain are obtained from the constitutive equation (E4) in Appendix E as $\tau_{rr}[\omega] = -2G^*(\omega)\frac{\partial u_r[\omega]}{\partial r}$ and $\tau_{r\theta}[\omega] = -G^*(\omega)(\frac{\partial u_\theta[\omega]}{\partial r} - \frac{u_\theta[\omega]}{r} + \frac{1}{r}\frac{\partial u_r[\omega]}{\partial\theta})$. The pressure is derived from Eq. (E6) as $p[\omega] = \text{const} + \frac{G^*(\omega)b(\omega)k(\omega)^2}{r^2}\cos\theta$. As a result, due to the linearity of the equation, the resistance force on the bead with the displacement $\delta\boldsymbol{r}_b[\omega]$ in the

frequency domain is obtained from these quantities as

$$\begin{aligned}\boldsymbol{F}[\omega] &= 2\pi R^2 \int_0^\pi [(-\tau_{rr}[\omega] - p[\omega])\cos\theta \\ &\quad + \tau_{r\theta}[\omega]\sin\theta]_{r=R}\sin\theta d\theta \\ &= -\left\{\frac{6\pi R G^*(\omega)}{i\omega} + 6\pi R^2\sqrt{\rho G^*(\omega)} + \frac{2}{3}\pi R^3\rho i\omega\right\} \\ &\quad \times i\omega\delta\boldsymbol{r}_{\rm b}[\omega]. \end{aligned} \tag{27}$$

The resistance force in fluids also has the same form [10]. The part in curly brackets of the last equation gives the Stokes component of the IGSER. The first term is the ordinary Stokes component of the inertialess GSER, the second term is friction from the Basset force [27] (referred to as the Basset friction) explained in Sec. VI, and the third term is the inertia of the medium dragged around with the bead [26,28]. Although the "Basset force" in the frequency domain was first derived by Stokes [29], we follow the conventional expression.

The following two modifications are required to obtain an appropriate form of the Stokes component of the IGSER.

(i) As explained in Sec. III, the contribution from a purely elastic component with elasticity $g_{\rm e} = H_{\rm e}/(6\pi R)$ already exists in the Einstein part as the frequency matrix $H_{\rm e} = 6\pi R g_{\rm e}$ outside of the memory function. Therefore the term $H_{\rm e}/(i\omega) = 6\pi R g_{\rm e}/(i\omega)$ must be subtracted from the memory function to derive a proper Stokes component. Otherwise one would double-count the contribution from the purely elastic element (both from the elastic term and from the memory function), and also an unphysical part that never decays would exist in the long-time limit of the memory function as well as the autocorrelation of the random force. Actually, our one-dimensional example showed that the pure elasticity should not be in the memory function (7).[1] On the other hand, the contribution from the purely elastic component remains in the Basset friction as we showed in the one-dimensional system where the Basset friction was $2\sqrt{\rho G}$, not 0.

(ii) It is convenient to subtract the contribution from the medium mass dragged around with the bead from the memory function and add it to the bare bead mass m in the Einstein component, Eq. (16). Then m in Eq. (16) is replaced with an effective bead mass $m_{\rm eff} := m + M/2$ with $M := \frac{4}{3}\pi R^3\rho$ being the medium mass per bead volume.

As a consequence of the modifications (i) and (ii) to Eq. (27), the Stokes component of the IGSER is expressed in terms of the memory function as

$$\begin{aligned}\bar{\zeta}[\omega] &= \frac{6\pi R[G^*(\omega) - g_{\rm e}]}{i\omega} + 6\pi R^2\sqrt{\rho G^*(\omega)} \\ &= -\frac{H_{\rm e}}{i\omega} + \frac{6\pi R G^*(\omega)}{i\omega} + 6\pi R^2\sqrt{\rho G^*(\omega)}. \end{aligned} \tag{28}$$

B. Two length scales of a viscoelastic medium

The real part $k'(\omega)$ and the imaginary part $k''(\omega)$ of the complex wave number $k(\omega) = -\omega\sqrt{\rho/G^*(\omega)}$ appearing in the displacement field can be expressed as

$$\begin{aligned} k'(\omega) &= -\omega\sqrt{\rho/|G^*(\omega)|}\cos[\Theta(\omega)/2], \\ k''(\omega) &= \omega\sqrt{\rho/|G^*(\omega)|}\sin[\Theta(\omega)/2], \end{aligned} \tag{29}$$

respectively, where we set $G^*(\omega) = |G^*(\omega)|e^{i\Theta(\omega)}$ [1]. Note that $k'(\omega)$ is negative (assuring the outward radiation) and $k''(\omega)$ is positive (satisfying the decaying condition), and also the inequality $|k'(\omega)| \geqslant k''(\omega)$ holds for all ω since the phase $\Theta(\omega)$ is defined at $[0,\pi/2]$. A term $e^{ik(\omega)r} = e^{i[k'(\omega)+ik''(\omega)]r} = e^{-ir/\Lambda(\omega)}e^{-r/\Delta(\omega)}$ in the displacement field describes the damped oscillation of the transverse sound wave or shear wave [1, p. 121] (see Fig. 5), where

$$\begin{aligned}\Lambda(\omega) &:= \frac{1}{|k'(\omega)|} = \frac{\sqrt{|G^*(\omega)|/\rho}}{\omega\cos[\Theta(\omega)/2]} \\ &= \frac{|G^*(\omega)|}{\omega}\sqrt{\frac{2}{\rho}\frac{1}{|G^*(\omega)| + G'(\omega)}} \end{aligned} \tag{30}$$

is the wavelength and

$$\begin{aligned}\Delta(\omega) &:= \frac{1}{k''(\omega)} = \frac{\sqrt{|G^*(\omega)|/\rho}}{\omega\sin[\Theta(\omega)/2]} \\ &= \frac{|G^*(\omega)|}{\omega}\sqrt{\frac{2}{\rho}\frac{1}{|G^*(\omega)| - G'(\omega)}} \end{aligned} \tag{31}$$

is the penetration depth (or length) of the shear wave penetrating into the medium from the bead surface [30]. The inequality $\Delta(\omega) \geqslant \Lambda(\omega)$ holds for all frequencies and all materials. If the medium is a purely viscous fluid ($\Theta(\omega) = \pi/2$), the equality $\Delta(\omega) = \Lambda(\omega)$ is attained, i.e., there is only a single length scale [see Fig. 5(a)]. If the medium is a purely elastic solid [$\Theta(\omega) = 0$], then $\Lambda(\omega)$ is finite but $\Delta(\omega)$ is infinity, so that there is also only a single length scale [Fig. 5(b)]. For a general viscoelastic material [$0 < \Theta(\omega) < \pi/2$], there are two length scales [Fig. 5(c)]. In the limit of no inertia of the medium ($\rho \to 0$), $k(\omega)$ goes to 0 and therefore both $\Lambda(\omega)$ and $\Delta(\omega)$ go to infinity, i.e., shear waves are not excited in the medium in the absence of medium inertia. The low-frequency behavior of the length scales is very different depending on the state of the medium. For viscoelastic fluids, each component of the dynamic modulus is $G' \sim \omega^2$, $G'' \sim \omega$ at the low-frequency terminal zone, so that $\Delta(\omega) \simeq \Lambda(\omega) \sim \omega^{-1/2}$. On the other hand, for viscoelastic solids, $\Delta(\omega)$ is much larger than $\Lambda(\omega)$ at low frequencies. Typically, both length scales are decreasing functions of ω in frequency overall (see Fig. 6).

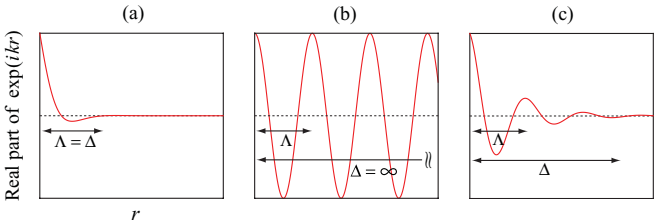

FIG. 5. (Color online) Schematic representations of shear waves propagating in a purely viscous fluid (a), a purely elastic solid (b), and a viscoelastic material (c).

[1] If we describe the Stokes component of the IGSER (or GSER) in terms of the complex compliance, the purely elastic term remains in the compliance.

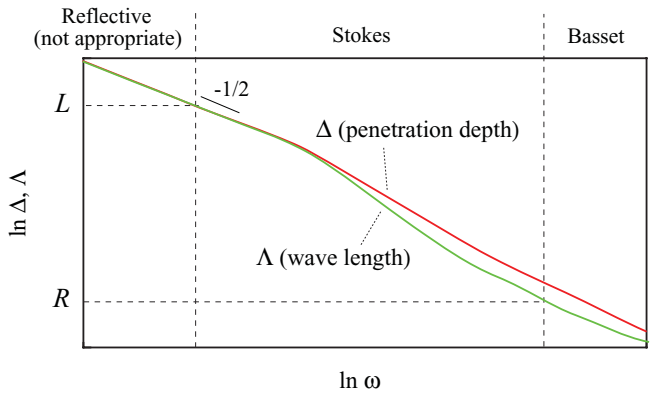

FIG. 6. (Color online) Penetration depth $\Delta(\omega)$ and wavelength $\Lambda(\omega)$ as functions of frequency for typical viscoelastic fluids. The Basset force becomes important at high frequencies satisfying the condition $\Lambda(\omega) \lesssim R$ for the particle radius R. On the other hand, reflection of the elastic waves from the medium boundary becomes effective at low frequencies satisfying $L \gtrsim \Delta(\omega)$ for the sample size L.

V. IGSER FOR FLUIDS AND SOLIDS

Before we interpret these results and explain the Basset force, we summarize how the Einstein part and the Stokes part derived above comprise the IGSER.

A. Forward representation

By replacing the bare bead's mass m in Eq. (16) with an effective bead mass $m_{\rm eff}$, the Einstein component is now written as

$$\left\langle \overline{\Delta\delta r_{\rm b}^2}[\omega] \right\rangle_{\rm eq} = \frac{6k_{\rm B}T}{i\omega(H_{\rm e} + i\omega\overline{\zeta}[\omega] - m_{\rm eff}\omega^2)}. \tag{32}$$

On the other hand, the Stokes component is expressed by Eq. (28), or

$$H_{\rm e} + i\omega\overline{\zeta}[\omega] = 6\pi R G^*(\omega) + 6\pi R^2 i\omega\sqrt{\rho G^*(\omega)}. \tag{33}$$

By the elimination of $H_{\rm e} + i\omega\overline{\zeta}[\omega]$ in these equations, we obtain the forward representation of the IGSER as

$$\left\langle \overline{\Delta\delta r_{\rm b}^2}[\omega] \right\rangle_{\rm eq} = \frac{6k_{\rm B}T}{i\omega[6\pi R G^*(\omega) + 6\pi R^2 i\omega\sqrt{\rho G^*(\omega)} - m_{\rm eff}\omega^2]}. \tag{34}$$

Here "forward" indicates that the MSD is obtained as a functional of $G^*(\omega)$. The power spectral density is given by calculating $I(\omega) = -{\rm Re}\{\langle\overline{\Delta\delta r_{\rm b}^2}[\omega]\rangle_{\rm eq}\}$.

B. Inverse representation

By inverting Eq. (32), the Einstein component is rewritten as

$$H_{\rm e} + i\omega\overline{\zeta}[\omega] = \frac{6k_{\rm B}T}{i\omega\left\langle \overline{\Delta\delta r_{\rm b}^2}[\omega] \right\rangle_{\rm eq}} + m_{\rm eff}\omega^2. \tag{35}$$

On the other hand, Eq. (28) is a quadratic equation in terms of $\sqrt{G^*(\omega)}$. By solving Eq. (28) for $\sqrt{G^*(\omega)}$ and then squaring the result, the Stokes component becomes

$$G^*(\omega) = \frac{H_{\rm e} + i\omega\overline{\zeta}[\omega]}{6\pi R} + \frac{R^2\omega^2}{2} \times \left(\sqrt{\rho^2 + \frac{2\rho}{3\pi R^3}\frac{H_{\rm e} + i\omega\overline{\zeta}[\omega]}{(i\omega)^2}} - \rho \right). \tag{36}$$

Signs were selected so that G' and G'' take positive values in the appropriate frequency range. The inverse expression of the IGSER which yields the dynamic modulus from the MSD is derived by eliminating $H_{\rm e} + i\omega\overline{\zeta}[\omega]$ in Eqs. (35) and (36) as

$$G^*(\omega) = \frac{k_{\rm B}T}{\pi R i\omega\left\langle \overline{\Delta\delta r_{\rm b}^2}[\omega] \right\rangle_{\rm eq}} + \frac{m_{\rm eff}\omega^2}{6\pi R} + \frac{R^2\omega^2}{2} \times \left[\sqrt{\rho^2 + \frac{2\rho}{3\pi R^3}\left(\frac{6k_{\rm B}T}{(i\omega)^3\left\langle \overline{\Delta\delta r_{\rm b}^2}[\omega] \right\rangle_{\rm eq}} - m_{\rm eff} \right)} - \rho \right]. \tag{37}$$

The first term on the right-hand side is the conventional GSER. The other terms are contributions from inertia.

It might be convenient in practice to separate the real and imaginary parts of the inverse expression of the IGSER (37). The storage modulus G' and the loss modulus G'' of the medium can be expressed as functions of the Fourier cosine transform $r'(\omega) := \int_0^\infty \langle\Delta\delta r_{\rm b}^2(t)\rangle_{\rm eq}\cos(\omega t)dt$ and the sine transform $r''(\omega) := -\int_0^\infty \langle\Delta\delta r_{\rm b}^2(t)\rangle_{\rm eq}\sin(\omega t)dt$ of the MSD in the forms

$$G'(\omega) = \frac{\gamma'(\omega)}{6\pi R} + \frac{R^2\omega^2}{2} \times \left(\sqrt{\frac{\beta'(\omega) + \sqrt{\beta'^2(\omega) + \beta''^2(\omega)}}{2}} - \rho \right), \tag{38a}$$

$$G''(\omega) = \frac{\gamma''(\omega)}{6\pi R} + \frac{R^2\omega^2}{2} \times \sqrt{\frac{-\beta'(\omega) + \sqrt{\beta'^2(\omega) + \beta''^2(\omega)}}{2}}, \tag{38b}$$

where β and γ are respectively defined by

$$\beta'(\omega) := \rho^2 - \frac{2\rho\gamma'(\omega)}{3\pi R^3\omega^2}, \tag{39a}$$

$$\beta''(\omega) := -\frac{2\rho\gamma''(\omega)}{3\pi R^3\omega^2}, \tag{39b}$$

and

$$\gamma'(\omega) := -\frac{6k_{\rm B}T}{\omega}\frac{r''(\omega)}{r'^2(\omega) + r''^2(\omega)} + m_{\rm eff}\omega^2, \tag{40a}$$

$$\gamma''(\omega) := -\frac{6k_{\rm B}T}{\omega}\frac{r'(\omega)}{r'^2(\omega) + r''^2(\omega)}. \tag{40b}$$

All equations in this section are also valid for fluids without modification except that the deviation $\delta\boldsymbol{r}_{\rm b}$ from the center of oscillation is replaced with the bead's location (or the displacement from an arbitrarily chosen origin) $\boldsymbol{r}_{\rm b}$. Note that $H_{\rm e} = 0$ for fluids, but $H_{\rm e}$ does not appear explicitly in the IGSER (or GSER) itself even for solids because $H_{\rm e}$ and $\overline{\zeta}[\omega]$ always appear as the combination $H_{\rm e} + i\omega\overline{\zeta}[\omega]$ in the Einstein part and the Stokes part, and these quantities ($H_{\rm e}$ and $\overline{\zeta}[\omega]$)

are eliminated simultaneously to derive the IGSER (or GSER) from these two parts.

VI. BASSET FORCE

Here we show in general that the Basset force is the frictional force associated with the energy dissipation of the bead by the radiation of shear waves that are excited by the vibrating bead but never return to the bead. As we did for the one-dimensional example in Sec. II B, we estimate the rate of energy transfer [21] arising from a harmonically oscillating embedded bead with the displacement $\boldsymbol{\epsilon} e^{i\omega t}$. The rate of energy transfer past a spherical boundary with radius r_0 is given as the surface integral of the work done by the medium on a unit area per time over the boundary:

$$P(r_0) = -\oint \dot{\boldsymbol{u}}[\omega] \cdot (-\boldsymbol{\tau}[\omega] - p[\omega]\boldsymbol{\delta}) \cdot d\boldsymbol{S} \tag{41}$$

$$= -2\pi r_0^2 \int_0^\pi \{(-\tau_{rr}[\omega] - p[\omega])\dot{u}_r[\omega] - \tau_{r\theta}[\omega]\dot{u}_\theta[\omega]\} \times \sin\theta d\theta. \tag{42}$$

The stress, pressure, and displacement field of the medium caused by such a harmonically oscillating bead are the same as those derived above for the Fourier component of an arbitrary small-displacement when the boundary condition is given by $\boldsymbol{u}[\omega] = \boldsymbol{\epsilon} e^{i\omega t}$ at the bead surface, and the energy flow can be obtained by substituting these quantities into Eq. (42). We chose a spherical boundary just for convenience although the displacement field is not spherically symmetric. This choice gives rise to somewhat artificial terms in P due to a mismatch of the form of the appropriate boundary (determined by the wave surface) and the spherical boundary.[2] The results from both boundaries must agree when the boundaries are sufficiently far from the bead position where these artificial terms decay.

A. Purely elastic solid

If the medium is an infinitely large purely elastic solid with modulus $G^*(\omega) = G$, then the wavelength of the shear wave $\Lambda(\omega) = \frac{\sqrt{G}}{\omega\sqrt{\rho}} = \frac{C}{\omega}$ is finite but the penetration depth is infinite [Fig. 5(a)] because the waves do not decay due to the absence of viscous elements in the medium. Therefore, the rate of energy transfer [Eq. (42)] has a finite value even at the boundary infinitely far from the bead position, i.e.,

$$P(r_0) = 6\pi R^2\sqrt{\rho G}\dot{u}(R,t-(r_0-R)/C)^2 \quad (r_0 \to \infty) \tag{43}$$

where $\dot{u}(R,t-(r_0-R)/C) = i\omega\epsilon e^{i\omega t}e^{-i(r_0-R)/\Lambda(\omega)}$. Equation (43) should correspond to the energy $\zeta_B \dot{u}(R,t)^2$ that the bead loses per unit time due to the radiation of the shear wave into the medium, where ζ_B is the friction associated with this radiational energy dissipation. By comparing the two expressions, we find that ζ_B is equal to the Basset friction $6\pi R^2\sqrt{\rho G}$ derived in Eq. (27). The time lags by $(r_0 - R)/C$ because it takes the time $(r_0 - R)/C$ for the wave to propagate from the bead surface to the boundary. Thus we know that the Basset force is the frictional force associated with the radiational energy dissipation of the bead toward the infinite boundary as discussed in Sec. II for a one-dimensional system. Purely elastic solids must have infinite dimension so that the bead can completely dissipate its energy because the wave reflected from the surface of the medium is absent and never returns to the bead in this case.

B. Voigt solid

If there is a small amount of viscosity η_0 in the solid, i.e., $G^*(\omega) = G + i\omega\eta_0$ with $\eta_0\omega/G \ll 1$, the wavelength is approximately the same as that of the purely elastic solid $\Lambda(\omega) \simeq \frac{\sqrt{G}}{\omega\sqrt{\rho}}$ but the penetration depth has a finite value $\Delta(\omega) \simeq \frac{2G^{3/2}}{\omega^2\eta_0\sqrt{\rho}}$ depending on the viscosity in the solid (called the Voigt solid). The penetration depth diverges in the limit of low viscosity, as it should. A small amount of viscosity can dissipate the wave's energy as it propagates, so that a finite sample size is possible, without the waves returning to the particle. In other words, the sample size L must satisfy $L \gg \frac{2G^{3/2}}{\omega^2\eta_0\sqrt{\rho}}$.

C. General viscoelastic materials

In general, the shear waves are damped in a viscoelastic medium by a viscous (or loss) component of the medium [Fig. 5(c)]. If the distance between the bead and medium surface is greater than the penetration depth $\Delta(\omega)$, then the wave excited by the bead decays before it reaches the surface and therefore there are no reflected waves from the medium surface. Thus, the sample size L must be much greater than the penetration depth $\Delta(\omega)$ in order to measure bulk rheology properly in microrheology as well as in mechanical rheology [30]. For viscoelastic fluids, the penetration depth $\Delta(\omega) \sim 1/\omega^{1/2}$ increases with decreasing frequency, so that larger medium size is required at lower frequencies (see Fig. 6).

As explained in Eq. (43) for purely elastic solids, the ratio of the rate of energy transfer $P(r_0)$ and the squared velocity $\dot{u}(R,t-(r_0-R)/C)^2$ provides the friction associated with the radiational energy dissipation. The same goes for viscoelastic media, although the radiated energy decays due to the Stokes-type dissipation by the viscous elements of the medium. From Eq. (42), we have

$$P(r_0)/\dot{u}(R,t-(r_0-R)/C(\omega))^2 = 6\pi R^2\sqrt{\rho G^*(\omega)} \quad (r_0 \to \infty). \tag{44}$$

This quantity $6\pi R^2\sqrt{\rho G^*(\omega)}$ is equal to the Basset friction derived in Eq. (27), so that we can conclude that even for a viscoelastic medium the Basset force is a frictional force associated with the radiational energy dissipation of the bead.

The wavelength $\Lambda(\omega)$ given by Eq. (30) can be a good indicator to estimate whether or not the Basset force is effective at a given frequency, i.e., if the frequency is high and therefore the wavelength is smaller than the particle size, $R \gtrsim \Lambda(\omega)$, then the Basset force is effective. The penetration depth $\Delta(\omega)$ of viscoelastic materials is often below 1 μm in the megahertz

[2]These terms are $2\pi R^2 G^* k\epsilon^2\omega e^{2i\omega t}\{-3e^{2ik(r_0-R)}[18i(kr_0)^{-5} + 36(kr_0)^{-4} - 31i(kr_0)^{-3} - 14kr_0^{-2} + 4i(kr_0)^{-1}] + e^{ik(r_0-R)}[-3 + 3ikR + (kR)^2][-36i(kr_0)^{-5} - 36(kr_0)^{-4} + 13i(kr_0)^{-3} + (kr_0)^{-2}] - 6i(kr_0)^{-5}[-3 + 3ikR + (kR)^2]^2\}$.

range, so that a sample volume of a few microliters is sufficient to satisfy the no-reflection condition of the shear wave $L \gg \Delta(\omega)$ at this high frequency [30]. On the other hand, medium inertia may be important in this high-frequency regime since the wavelength is always smaller than the penetration depth and therefore $\Lambda(\omega)$ can be smaller than the bead size R of order micrometers. See Fig. 6 for reference.

VII. COMPETING EFFECTS OF BEAD INERTIA AND MEDIUM INERTIA

As explained in Sec. III C, the bead's inertia gives rise to oscillations in the MSD because of the resonance between the inertial motion of the bead and the elastic component of the medium. The oscillation can be attenuated if there is a purely viscous element in the medium to dissipate the bead's energy [10,24]. Medium inertia can also attenuate the MSD's oscillation through the Basset force because the Basset force plays the same role as the viscous component due to the dissipation of the bead's energy by the radiation of elastic waves excited by the bead's vibration. Thus, bead inertia competes with medium inertia for the generation of the MSD's oscillation, even in the absence of a purely viscous element. We here derive a sufficient condition that the oscillation of the MSD (or, equivalently, the peak in the PSD) does *not* occur as a result of the competition between bead inertia and medium inertia.

In general, the dynamic modulus of a viscoelastic material without purely viscous elements can be expressed by the generalized Maxwell model

$$G^*(\omega) = g_e + \sum_{j=1}^{N} g_j \frac{i\omega\lambda_j}{1+i\omega\lambda_j}, \tag{45}$$

where g_e is the static modulus of the purely elastic element, i.e., the elastic component that remains in the zero-frequency limit, g_j and λ_j are the modulus and the relaxation time, respectively, of the jth Maxwell element, and N is the number of relaxation modes. The effects of the purely viscous element are considered later. The memory function is then obtained by putting Eq. (45) into Eq. (28) as

$$\bar{\zeta}[\omega] = \sum_j H_j \frac{\lambda_j}{1+i\omega\lambda_j} + \frac{3\sqrt{M}}{\sqrt{2}} \sqrt{H_e + \sum_j H_j \frac{i\omega\lambda_j}{1+i\omega\lambda_j}}, \tag{46}$$

where $H_e = 6\pi R g_e$ and $H_j = 6\pi R g_j$ as before. We first consider high-frequency regimes $\omega \gg 1/\lambda_j$ for all $j = 1,2,\ldots,N$ because the oscillation of the MSD originates from the elasticity of the medium, and therefore the frequency of the oscillation tends to be around there, where the elasticity of the medium is dominant. A generalization of the result is discussed below. In this high-frequency regime, $i\omega\lambda_j/(1+i\omega\lambda_j) \simeq 1$ for all j, so that Eq. (46) is approximately written as

$$H_e + i\omega\bar{\zeta}[\omega] \simeq \left(H_e + \sum_j H_j\right)(1 + i\omega/\omega_M), \tag{47}$$

where

$$\omega_M := \frac{\sqrt{2}}{3}\sqrt{\frac{H_e + \sum_j H_j}{M}} \tag{48}$$

is the frequency above which the Basset force becomes effective. We assume that the fluid density ρ (or mass M) is so small as to satisfy the condition $\omega_M \gg 1/\lambda_j$ for all j. Equation (47) is correct up to the zeroth order of $1/\omega$ and $1/\omega_M$. Putting Eq. (47) into Eq. (32), the MSD in the frequency domain is approximately derived as

$$\left\langle \overline{\Delta\delta r_b^2}[\omega] \right\rangle_{eq} \simeq \frac{6k_BT}{m_{eff}} \frac{(i\omega)^2 - \phi\omega_M i\omega + \phi\omega_M^2}{i\omega[(i\omega)^2 - 1/\tau_+^2][(i\omega)^2 - 1/\tau_-^2]}, \tag{49}$$

where

$$\phi := \frac{9M}{2m_{eff}}, \tag{50}$$

and

$$1/\tau_\pm^2 := (\phi/2-1)\phi\omega_M^2 \pm \sqrt{\left[(\phi/2-1)\phi\omega_M^2\right]^2 - \left(\phi\omega_M^2\right)^2} \tag{51}$$

determines the poles of Eq. (49). If $\phi > 2$, or

$$\frac{M}{m}\left(=\frac{\rho}{\rho_b}\right) > \frac{4}{7}, \tag{52}$$

then $\tau_\pm^2$ is positive, so that all poles are real, indicating that the MSD does not oscillate at frequencies $\omega \gg 1/\min\{\lambda_j\}$.

The oscillation of the MSD can also be identified as a peak in the PSD. The PSD is obtained by taking the real part of Eq. (49) under the same condition $\omega, \omega_M \gg 1/\lambda_j$ for all j, i.e.,

$$\begin{aligned} I(\omega) &= -\mathrm{Re}\left\{\left\langle \overline{\Delta\delta r_b^2}[\omega] \right\rangle_{eq}\right\} \\ &\simeq \frac{6k_BT}{m_{eff}} \frac{\phi\omega_M}{(\omega^2 - \phi\omega_M^2)^2 + (\phi\omega_M\omega)^2} \qquad (53) \\ &= \frac{6k_BT}{m_{eff}} \frac{\phi\omega_M}{\left[\omega^2 + \frac{1}{2}(\phi-2)\phi\omega_M^2\right]^2 + (1-\frac{\phi}{4})\phi^3\omega_M^4}. \qquad (54) \end{aligned}$$

If $\phi > 2$, or inequality (52) is satisfied, the denominator of Eq. (54) is a monotonically increasing function of ω, and therefore the peak does not occur in the PSD at $\omega \gg 1/\min\{\lambda_j\}$.

Figure 7 compares the approximate PSD given by Eq. (54) and the rigorous one for the Rouse model ($g_j = g_1$ for all j and $\lambda_j = \lambda_1/j^2$) as a standard example. The two agree at $\omega \gg 1/\min\{\lambda_j\} = N^2/\lambda_1$ as expected. As seen in Fig. 7(a), the relative peak height (from the initial rise) of the approximate PSD is higher than that of the rigorous PSD. This error comes from the assumption $\omega \gg 1/\min\{\lambda_j\}$ that we employed. In this assumption, the storage modulus of each mode $G'_j := g_1(\omega\lambda_j)^2/[1+(\omega\lambda_j)^2]$ is replaced with g_1 for all ω, and therefore G'_j is overestimated for all j. Since the peak of the PSD (or the oscillation of the MSD) originates from the resonance between the inertial motion of the bead and the elastic element of the medium as discussed in Sec. III C, the overestimation of the storage modulus leads to

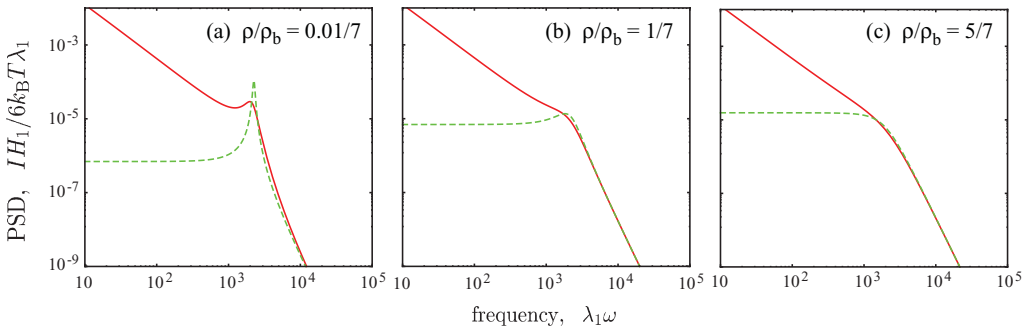

FIG. 7. (Color online) Power spectral density for the Rouse model with 50 modes. Solid lines indicate rigorous PSD, and dotted lines represent approximate PSD. (a) Both rigorous PSD and approximate PSD show a peak; (b) the rigorous PSD does not exhibit a peak while the approximate PSD does; (c) both rigorous PSD and approximate PSD show no peak. $g_e = 0$, $m = 10^{-5}\lambda_1^2 H_1$.

the overestimation of the peak height. As a result, the absence of a peak in the approximate PSD guarantees that no peak will arise in the exact PSD. Therefore, we can say in general that if condition (52) is satisfied, the peak never appears in the (exact) PSD for all ω, as seen in Fig. 7(c), or, equivalently, the (exact) MSD does not oscillate, independent of the details of the relaxation spectrum. This holds even in the presence of a purely viscous element which always attenuates the oscillation further.

It should be emphasized that even if condition (52) is *not* satisfied, or $\frac{\rho}{\rho_b} < \frac{4}{7}$, the MSD does not necessarily oscillate [see Fig. 7(b)]. Whether or not the oscillation occurs in the MSD when $\frac{\rho}{\rho_b} < \frac{4}{7}$ depends on the relaxation spectrum of the material. Therefore Eq. (52) is a sufficient condition for the oscillation in the MSD not to occur. However, for a purely elastic solid, Eq. (52) is a sufficient and necessary condition for MSD oscillation not to occur, i.e., the MSD does not oscillate when $\frac{\rho}{\rho_b} > \frac{4}{7}$ but it oscillates when $\frac{\rho}{\rho_b} < \frac{4}{7}$. Also, even for a single-mode Maxwell fluid, Eq. (52) is a sufficient and necessary condition to a very good approximation. (If the relaxation time is $\lambda \simeq 10^{-1} - 10$ s as typical Maxwell fluids [31,32] while $1/\omega_M \simeq 10^{-6} \sim 10^{-5}$ s [10], then the condition $\omega_M \gg 1/\lambda$ is adequately satisfied.) We were less specific about this condition (52) in our recent paper [10]. In Ref. [10], only a single-mode Maxwell fluid is considered and the condition (52) is not specified; we said that the oscillation is attenuated if the bead density and medium density are comparable.

When the number of modes is larger, oscillation in the MSD is less likely to appear even if $\frac{\rho}{\rho_b} < \frac{4}{7}$. This fact has been indicated in Ref. [13] for arbitrary N and in our paper [10] for $N = 2$ when medium inertia is neglected and the purely viscous element is absent. Also, if $\min\{\lambda_j\} = 0$, then the oscillation never appears even if the number of modes is finite, as shown in our paper [10] for two-mode Maxwell fluids.

In spite of this limitation, condition (52) for the oscillation not to occur can explain an important experimental fact. In typical microrheological measurements, the fluid density ρ and bead density ρ_b are comparable so that the bead neither floats nor sinks. If $\rho_b = \rho$, the condition (52) is satisfied. This is one possible reason why the MSD's oscillations due to inertial effects have not been observed experimentally for viscoelastic systems (without an external force to trap the bead) studied so far. It is also interesting to note that the sufficiency condition (52) is determined only by the ratio of the medium density ρ and the bead density ρ_b, irrespective of details of the relaxation spectrum of the medium. Intuitively, one can understand this independence of details of $G^*(\omega)$ by recognizing that increases in g_e contribute simultaneously to elasticity in the Stokes term, and damping in the Basset term.

The oscillation condition (52) is applicable to both fluids and solids.

VIII. A BEAD IN A FLUID TRAPPED BY AN EXTERNAL FORCE

Before concluding this article, it is worth considering a different but relevant system where a tracer bead is embedded in a viscoelastic *fluid* but is trapped by a static external force $\boldsymbol{f}_{\rm ext}(\delta \boldsymbol{r}_b)$ (e.g., optical tweezers [5]). Usually, the external force can be approximated linearly, i.e., $\boldsymbol{f}_{\rm ext}(\delta \boldsymbol{r}_b) = -H_e \delta \boldsymbol{r}_b$, where the proportionality coefficient H_e represents the strength of the trap in this case. The bead in this system obeys the same GLE as Eq. (12), although H_e is a parameter here, and therefore the bead's MSD in the frequency domain is given by Eq. (32). The medium is a fluid, so that nothing should be subtracted from the memory function, unlike in Eq. (28), i.e.,

$$\bar{\zeta}[\omega] = \frac{6\pi R G^*(\omega)}{i\omega} + 6\pi R^2 \sqrt{\rho G^*(\omega)}. \tag{55}$$

Therefore, the IGSER of this system is given as the set of equations (55) and (32) for the forward expression or Eq. (36) for the inverse expression (but now H_e is the trap strength).

In the presence of an external force to trap the bead, even if inequality (52) is satisfied, the MSD can oscillate when the trap intensity H_e is large. This is because the trap force intensifies the resonance with the bead's motion but does not affect the Basset damping. Actually, we can confirm that the relative peak height of the PSD for viscoelastic fluids increases with H_e as experimentally observed for Newtonian fluids [33]. These results are different from results for viscoelastic solids for which, if inequality (52) is satisfied, the peak never appears in the PSD no matter how large the elasticity g_e [$= H_e/(6\pi R)$] of the purely elastic component is. Thus the effects of the

external force in trapping the bead and those of the purely elastic component of the medium are not equivalent.

The IGSER can also treat nonlinear and nonconservative external forces [34] trapping the bead [24].

IX. SUMMARY AND CONCLUSION

In this paper, we obtained the following results. (i) We derived a relation (which we call the IGSER) that estimates $G^*(\omega)$ from the MSD and vice versa for viscoelastic solids, including inertial effects of both bead and medium. It turns out to be the same as the IGSER for viscoelastic fluids; (ii) We provided a rigorous justification of passive microrheology for purely elastic solids by considering the medium inertia which brings about radiational energy dissipation via the Basset force. (iii) We found a sufficient condition that the MSD of the bead in a viscoelastic medium (solid and fluid) does not oscillate in the absence of an external force to trap the bead. These items are summarized as follows.

(i) The dynamics of a bead in viscoelastic solids is described by a GLE that includes a linear elastic term originating from the purely elastic component of the medium. The coefficient of the elastic term H_e corresponds to the so-called frequency matrix appearing in the projection-operator method. The Einstein part of the IGSER is obtained by solving the GLE, and therefore it contains the term H_e. On the other hand, the Stokes component is derived by solving the equation of motion for the displacement field of the medium containing a vibrating spherical bead. For solids, the purely elastic component H_e must be subtracted from the memory function in the Stokes component because it already exists in the Einstein component. Thus, in spite of the presence of the purely elastic component, the IGSER for solids has a form identical to that for fluids.

Item (ii) is motivated by an intuitively plausible but unsatisfactory observation: a bead embedded in a purely elastic solid cannot lose its energy by dissipation of the Stokes type, and therefore cannot fluctuate because of the fluctuation-dissipation theorem, thereby leading to a breakdown of the GSER without inertia. We first studied a bead in a one-dimensional harmonic lattice and showed that elastic waves are excited in the medium by bead vibration, and the tagged bead's energy transfers along with the waves toward the medium boundaries. The elastic wave is reflected from the boundaries, giving periodic behavior in the memory function. If the medium boundaries are infinitely far from the bead, then the transmitted energy never returns to the bead, thereby leading to the dissipation of the bead's energy even in purely elastic solids. The Basset force of medium inertia is the frictional force associated with this radiational dissipation. We showed that the same goes for a spherical bead embedded in three-dimensional continuum purely elastic solids if the medium inertia is considered. Thus it is indispensable to take inertial effects into account for purely elastic solids to avoid the breakdown of the GSER. For viscoelastic solids, Stokes-type dissipation due to viscous components occurs in addition to the radiational dissipation, and therefore the elastic waves cannot travel beyond the penetration depth. If the medium size is much greater than the penetration depth, there are no reflected waves in the medium, so that bulk rheology can be properly estimated by passive microrheology as well as by the conventional mechanical rheology.

(iii) Bead inertia has the potential to bring about oscillation in the MSD due to resonance with the elastic part of the medium. The oscillations can be enhanced for solids due to the presence of a purely elastic component of the medium. On the other hand, medium inertia tends to attenuate the oscillation through the Basset force because of dissipation of the bead's energy due to the radiation of transverse shear waves as discussed in (ii). Thus, the bead inertia competes with the medium inertia to determine if there are oscillations in the MSD. By applying the IGSER derived in (i), we showed that the condition that the Basset damping suppresses the oscillation is determined only by the ratio of the medium density ρ to the bead density ρ_b, and the MSD is guaranteed not to oscillate for viscoelastic solids and fluids if $\rho/\rho_b > 4/7$. This is a sufficient condition for the oscillation not to occur, that is, the oscillation may not occur even if the opposite condition is satisfied; it depends on the relaxation spectrum of the medium. In spite of this limitation, the condition explains why the MSD's oscillations are not observed for viscoelastic materials.

ACKNOWLEDGMENTS

We are grateful to the Army Research Office (Grants No. W911NF-08-2-0058 and No. W911NF-09-1-0378) for financial support.

APPENDIX A: GENERALIZED LANGEVIN EQUATION

Here we outline the derivation of the GLE by the projection-operator method of Mori [16]. We consider an arbitrary-dimensional system of ν particles. The time development of this system is determined by the equation of motion, the initial momenta $\boldsymbol{p} := (\boldsymbol{p}_1, \ldots, \boldsymbol{p}_\nu)$, and the initial positions $\boldsymbol{r} := (\boldsymbol{r}_1, \ldots, \boldsymbol{r}_\nu)$ of all particles. An arbitrary physical variable $\boldsymbol{Y}(t) := \boldsymbol{Y}(\boldsymbol{p},\boldsymbol{r},t)$ obeys the following equation [14, Chap. 2]:

$$\frac{\partial \boldsymbol{Y}(t)}{\partial t} = i\mathcal{L}\boldsymbol{Y}(t), \tag{A1}$$

where $i\mathcal{L}$ is the Liouville operator of the system defined for the total Hamiltonian $\mathcal{H}$ as

$$i\mathcal{L} = -\frac{\partial \mathcal{H}}{\partial \boldsymbol{r}} \cdot \frac{\partial}{\partial \boldsymbol{p}} + \frac{\partial \mathcal{H}}{\partial \boldsymbol{p}} \cdot \frac{\partial}{\partial \boldsymbol{r}}. \tag{A2}$$

It is possible to divide the time development of $\boldsymbol{Y}(t)$ into two components; one is the part projected onto $\boldsymbol{Y} := \boldsymbol{Y}(0)$ and the other is the component orthogonal to $\boldsymbol{Y}$. This separation is conducted by applying the projection operator $\mathcal{P}$ to $\boldsymbol{Y}(t)$ onto $\boldsymbol{Y}$, defined by

$$\mathcal{P}\boldsymbol{Y}(t) := \langle \boldsymbol{Y}(t), \boldsymbol{Y} \rangle \cdot \langle \boldsymbol{Y}, \boldsymbol{Y} \rangle^{-1} \cdot \boldsymbol{Y}. \tag{A3}$$

The inner product $\langle , \rangle$ for arbitrary vector variables $\boldsymbol{B}$ and $\boldsymbol{C}$ is usually defined as the canonical averaging of a dyadic product at equilibrium, i.e.,

$$\langle \boldsymbol{B}, \boldsymbol{C} \rangle := \langle \boldsymbol{B}\boldsymbol{C} \rangle_{\mathrm{eq}} := \frac{1}{Z} \int d\boldsymbol{p} \int d\boldsymbol{r}\, \boldsymbol{B}\boldsymbol{C} e^{-\mathcal{H}/k_B T}, \tag{A4}$$

where $Z = \int d\boldsymbol{p} \int d\boldsymbol{r} e^{-\mathcal{H}/k_B T}$ is the canonical partition function. Equation (A1) is transformed into the form of a GLE by

this separation [14,16], i.e.,

$$\frac{d\boldsymbol{Y}(t)}{dt} = i\boldsymbol{\Omega}\cdot\boldsymbol{Y}(t) - \int_0^t \boldsymbol{\gamma}(t-t')\cdot\boldsymbol{Y}(t')dt' + \boldsymbol{F}(t). \quad \text{(A5)}$$

The first term in the right-hand side is the projected part of $d\boldsymbol{Y}(t)/dt$ onto $\boldsymbol{Y}$. The coefficient of $\boldsymbol{Y}(t)$ is called the frequency matrix and is defined by

$$i\boldsymbol{\Omega} = \langle\dot{\boldsymbol{Y}},\boldsymbol{Y}\rangle\cdot\langle\boldsymbol{Y},\boldsymbol{Y}\rangle^{-1}, \quad \text{(A6)}$$

where $\dot{\boldsymbol{Y}} := d\boldsymbol{Y}(t)/dt|_{t=0}$. The second and the third terms originate from the part of $d\boldsymbol{Y}(t)/dt$ normal to $\boldsymbol{Y}$. The second term is the memory integral representing the frictional resistance force with time retardation, and the third term is interpreted as the random force given by

$$\boldsymbol{F}(t) = e^{t\mathcal{D}i\mathcal{L}}\mathcal{D}i\mathcal{L}\boldsymbol{Y}, \quad \text{(A7)}$$

where the operator $\mathcal{D} := 1-\mathcal{P}$ projects onto the space normal to $\boldsymbol{Y}$. The random force is perpendicular to $\boldsymbol{Y}$ as it should be, i.e., $\langle\boldsymbol{F}(t),\boldsymbol{Y}\rangle = 0$. The memory-function matrix $\boldsymbol{\gamma}(t)$ is related to the autocorrelation function of the random force via the fluctuation-dissipation theorem of the second kind:

$$\boldsymbol{\gamma}(t) = \langle\boldsymbol{F}(t),\boldsymbol{F}\rangle\cdot\langle\boldsymbol{Y},\boldsymbol{Y}\rangle^{-1}. \quad \text{(A8)}$$

APPENDIX B: DERIVATION OF Eq. (2)

Here we derive the GLE (2) of the tagged bead embedded in the linear harmonic lattice as shown in Fig. 1. The total Hamiltonian is given by

$$\mathcal{H} = \frac{H_s}{2}\delta\boldsymbol{r}\cdot\boldsymbol{A}\cdot\delta\boldsymbol{r} + \frac{1}{2}\boldsymbol{p}\cdot\boldsymbol{M}^{-1}\cdot\boldsymbol{p}, \quad \text{(B1)}$$

where $\boldsymbol{A}$ is the $\nu\times\nu$ tridiagonal Rouse matrix defined by $A_{ij} := 1\ (i=j=1),\ 2\ (i=j\neq 1,\nu),\ -1\ (i=j\pm 1),\ 0\ (i\neq j, j\pm 1)$ [20], and $\boldsymbol{M}^{-1}$ is a diagonal inverse mass matrix defined by $M_{ij}^{-1} := 1/m\ (i=j=n),\ 1/\mu(i=j\neq n),\ 0\ (i\neq j)$. The evolution of the total system $\boldsymbol{X}(t) = (\boldsymbol{p}(t),\delta\boldsymbol{r}(t))$ is determined by the following equation [14]:

$$\frac{d\boldsymbol{X}(t)}{dt} = i\mathcal{L}\boldsymbol{X}(t), \quad \text{(B2)}$$

where the Liouville operator of the system is given by

$$\begin{aligned} i\mathcal{L} &= -\frac{\partial\mathcal{H}}{\partial\delta\boldsymbol{r}}\cdot\frac{\partial}{\partial\boldsymbol{p}} + \frac{\partial\mathcal{H}}{\partial\boldsymbol{p}}\cdot\frac{\partial}{\partial\delta\boldsymbol{r}} \\ &= -H_s\delta\boldsymbol{r}\cdot\boldsymbol{A}\cdot\frac{\partial}{\partial\boldsymbol{p}} + \boldsymbol{p}\cdot\boldsymbol{M}^{-1}\cdot\frac{\partial}{\partial\delta\boldsymbol{r}}. \end{aligned} \quad \text{(B3)}$$

The time argument is omitted when $t=0$ for simplicity. The operator $i\mathcal{L}$ operates on $\boldsymbol{X}(t)$ through its initial value $\boldsymbol{X}$. The equation of motion for the tagged bead is the nth element of Eq. (B2), i.e.,

$$\frac{d\boldsymbol{X}_n(t)}{dt} = i\mathcal{L}\boldsymbol{X}_n(t), \quad \text{(B4)}$$

where $\boldsymbol{X}_n(t) = (p_n(t),\ \delta r_n(t))$ is the two-dimensional vector that characterizes the tagged bead.

Equation (B2) is a linear ordinary differential equation and has the following solution:

$$\boldsymbol{X}(t) = \begin{pmatrix}\boldsymbol{p}(t)\\ \delta\boldsymbol{r}(t)\end{pmatrix} = \begin{pmatrix}\boldsymbol{a}(t)\cdot\boldsymbol{p} + \boldsymbol{b}(t)\cdot\delta\boldsymbol{r}\\ \boldsymbol{c}(t)\cdot\boldsymbol{p} + \boldsymbol{d}(t)\cdot\delta\boldsymbol{r}\end{pmatrix}, \quad \text{(B5)}$$

where $\boldsymbol{a}(t) := \cos(t\boldsymbol{g})$, $\boldsymbol{b}(t) := -H_s\sin(t\boldsymbol{g})\cdot\boldsymbol{g}^{-1}\cdot\boldsymbol{A}$, $\boldsymbol{c}(t) := \sin(t\boldsymbol{g}^\dagger)\cdot(\boldsymbol{g}^\dagger)^{-1}\cdot\boldsymbol{M}^{-1}$, and $\boldsymbol{d}(t) := \cos(t\boldsymbol{g}^\dagger)$ are $\nu\times\nu$ matrices and $\boldsymbol{g}$ is defined through $\boldsymbol{g}^2 = H_s\boldsymbol{A}\cdot\boldsymbol{M}^{-1}$. The solution for the tagged bead is the nth element of Eq. (B5), i.e.,

$$\boldsymbol{X}_n(t) = \begin{pmatrix}p_n(t)\\ \delta r_n(t)\end{pmatrix} = \begin{pmatrix}[\boldsymbol{a}(t)\cdot\boldsymbol{p} + \boldsymbol{b}(t)\cdot\delta\boldsymbol{r}]_n\\ [\boldsymbol{c}(t)\cdot\boldsymbol{p} + \boldsymbol{d}(t)\cdot\delta\boldsymbol{r}]_n\end{pmatrix}, \quad \text{(B6)}$$

and its time derivative is

$$\frac{d\boldsymbol{X}_n(t)}{dt} = i\mathcal{L}\boldsymbol{X}_n(t) = \begin{pmatrix}-[H_s\boldsymbol{A}\cdot\delta\boldsymbol{r}(t)]_n\\ \left[\boldsymbol{M}^{-1}\cdot\boldsymbol{p}(t)\right]_n\end{pmatrix} =: \begin{pmatrix}f(t)\\ v(t)\end{pmatrix}. \quad \text{(B7)}$$

The first component $f(t)$ is the force on the tagged bead and the second component $v(t)$ is the bead's velocity. By applying the projection-operator method of Mori [16], Eq. (B7) is transformed into the form of a GLE:

$$\frac{d\boldsymbol{X}_n(t)}{dt} = i\boldsymbol{\Omega}\cdot\boldsymbol{X}_n(t) - \int_0^t \boldsymbol{\gamma}(t-t')\cdot\boldsymbol{X}_n(t')dt' + \boldsymbol{F}(t). \quad \text{(B8)}$$

The projection-operator method is briefly explained in Appendix A. The random force $\boldsymbol{F}(t)$ on the tagged bead in the $(p_n,\delta r_n)$ space is defined by Eq. (A7). In the present case, it is given by

$$\boldsymbol{F}(t) = e^{t\mathcal{D}i\mathcal{L}}\mathcal{D}i\mathcal{L}\boldsymbol{X}_n. \quad \text{(B9)}$$

Equation (B9) can be calculated by making use of the exact solution for the total system [Eq. (B5)] as follows. First, by applying the Liouville operator given by Eq. (B3), the exact solution for the arbitrary lth bead,

$$\boldsymbol{X}_l(t) = \begin{pmatrix}p_l(t)\\ \delta r_l(t)\end{pmatrix} = \begin{pmatrix}[\boldsymbol{a}(t)\cdot\boldsymbol{p} + \boldsymbol{b}(t)\cdot\delta\boldsymbol{r}]_l\\ [\boldsymbol{c}(t)\cdot\boldsymbol{p} + \boldsymbol{d}(t)\cdot\delta\boldsymbol{r}]_l\end{pmatrix}, \quad \text{(B10)}$$

becomes

$$\begin{aligned} i\mathcal{L}\boldsymbol{X}_l(t) &= \begin{pmatrix}i\mathcal{L}p_l(t)\\ i\mathcal{L}\delta r_l(t)\end{pmatrix} \\ &= \begin{pmatrix}[-H_s\boldsymbol{a}(t)\cdot\boldsymbol{A}\cdot\delta\boldsymbol{r} + \boldsymbol{b}(t)\cdot\boldsymbol{M}^{-1}\cdot\boldsymbol{p}]_l\\ [-H_s\boldsymbol{c}(t)\cdot\boldsymbol{A}\cdot\delta\boldsymbol{r} + \boldsymbol{d}(t)\cdot\boldsymbol{M}^{-1}\cdot\boldsymbol{p}]_l\end{pmatrix}. \end{aligned} \quad \text{(B11)}$$

Next, by applying the projection operator defined by Eq. (A3) for $\boldsymbol{Y} = \boldsymbol{X}_n = (p_n,\delta r_n)$, the last equation reduces to

$$\begin{aligned} &\mathcal{P}i\mathcal{L}\boldsymbol{X}_l(t) \\ &= \begin{pmatrix}\langle[i\mathcal{L}p_l(t)]p_n\rangle_{\rm eq} & \langle[i\mathcal{L}p_l(t)]\delta r\rangle_{\rm eq}\\ \langle[i\mathcal{L}\delta r_l(t)]p_n\rangle_{\rm eq} & \langle[i\mathcal{L}\delta r_l(t)]\delta r_n\rangle_{\rm eq}\end{pmatrix}\begin{pmatrix}p_n/\langle(p_n)^2\rangle_{\rm eq}\\ \delta r_n/\langle(\delta r_n)^2\rangle_{\rm eq}\end{pmatrix} \\ &= \begin{pmatrix}\frac{b_{ln}(t)}{m}p_n - \frac{H_s a_{ln}(t)}{C_{nn}}\delta r_n\\ \frac{d_{ln}(t)}{m}p_n - \frac{H_s c_{ln}(t)}{C_{nn}}\delta r_n\end{pmatrix}, \end{aligned} \quad \text{(B12)}$$

where $\boldsymbol{C} = \boldsymbol{A}^{-1}$ is the Kramers matrix [20] and we have used the relations

$$\langle\delta r_i\delta r_j\rangle_{\rm eq} = \frac{k_{\rm B}T}{H_s}C_{ij},\quad \langle p_i p_j\rangle_{\rm eq} = mk_{\rm B}T\delta_{ij}. \quad \text{(B13)}$$

Therefore,

$$\mathcal{D}i\mathcal{L}\boldsymbol{X}_l(t) = i\mathcal{L}\boldsymbol{X}_l(t) - \mathcal{P}i\mathcal{L}\boldsymbol{X}_l(t) = \begin{pmatrix} [-H_s\boldsymbol{a}(t)\cdot\tilde{\boldsymbol{A}}\cdot\delta\boldsymbol{r} + \boldsymbol{b}(t)\cdot\tilde{\boldsymbol{M}}^{-1}\cdot\boldsymbol{p}]_l \\ [-H_s\boldsymbol{c}(t)\cdot\tilde{\boldsymbol{A}}\cdot\delta\boldsymbol{r} + \boldsymbol{d}(t)\cdot\tilde{\boldsymbol{M}}^{-1}\cdot\boldsymbol{p}]_l \end{pmatrix}, \tag{B14}$$

where $\tilde{\boldsymbol{A}}$ and $\tilde{\boldsymbol{M}}^{-1}$ are defined by

$$\tilde{A}_{ij} := A_{ij} - \frac{\delta_{in}\delta_{jn}}{C_{nn}} \tag{B15}$$

and

$$\tilde{M}^{-1}_{ij} := M^{-1}_{ij} - m^{-1}\delta_{in}\delta_{jn}, \tag{B16}$$

respectively. The (n,n) element of $\tilde{\boldsymbol{A}}$ is smaller than $\boldsymbol{A}$ by $1/C_{nn} = (\nu+1)/[n(\nu+1-n)]$. The other elements of $\tilde{\boldsymbol{A}}$ are equal to those of $\boldsymbol{A}$. On the other hand, the (n,n) element of $\tilde{\boldsymbol{M}}^{-1}$ is 0 and the other elements are μ^{-1}. At $t=0$, Eq. (B14) reduces to

$$\mathcal{D}i\mathcal{L}\boldsymbol{X}_l = \begin{pmatrix} \mathcal{D}i\mathcal{L}p_l \\ \mathcal{D}i\mathcal{L}\delta r_l \end{pmatrix} = \begin{pmatrix} -[H_s\tilde{\boldsymbol{A}}\cdot\delta\boldsymbol{r}]_l \\ [\tilde{\boldsymbol{M}}^{-1}\cdot\boldsymbol{p}]_l \end{pmatrix} \tag{B17}$$

because $\boldsymbol{a}(0) = \boldsymbol{d}(0) = \boldsymbol{\delta}$ and $\boldsymbol{b}(0) = \boldsymbol{c}(0) = \boldsymbol{0}$. Finally, by using Eq. (B17) iteratively, the following equations can be obtained for $j = 0,1,2,\ldots$:

$$t^{2j}(\mathcal{D}i\mathcal{L})^{2j+1}\boldsymbol{X}_n = \begin{pmatrix} (-1)^{j+1}[H_s\tilde{\boldsymbol{A}}\cdot(t\tilde{\boldsymbol{g}}^\dagger)^{2j}\cdot\delta\boldsymbol{r}]_n \\ (-1)^{j}[\tilde{\boldsymbol{M}}^{-1}\cdot(t\tilde{\boldsymbol{g}})^{2j}\boldsymbol{p}]_n \end{pmatrix}, \tag{B18}$$

$$t^{2j+1}(\mathcal{D}i\mathcal{L})^{2j+2}\boldsymbol{X}_n = \begin{pmatrix} (-1)^{j+1}[H_s\tilde{\boldsymbol{A}}\cdot(t\tilde{\boldsymbol{g}}^\dagger)^{2j+1}\cdot(\tilde{\boldsymbol{g}}^\dagger)^{-1}\cdot\tilde{\boldsymbol{M}}^{-1}\cdot\boldsymbol{p}]_n \\ (-1)^{j+1}[\tilde{\boldsymbol{M}}^{-1}\cdot(t\tilde{\boldsymbol{g}})^{2j+1}\cdot\tilde{\boldsymbol{g}}^{-1}\cdot H_s\tilde{\boldsymbol{A}}\cdot\delta\boldsymbol{r}]_n \end{pmatrix}, \tag{B19}$$

where the matrix $\tilde{\boldsymbol{g}}$ is defined by $\tilde{\boldsymbol{g}}^2 = H_s\tilde{\boldsymbol{A}}\cdot\tilde{\boldsymbol{M}}^{-1}$. Therefore, Eq. (B9) turns out to be

$$\boldsymbol{F}(t) = \sum_{j=0}^{\infty}\frac{t^{2j}}{(2j)!}(\mathcal{D}i\mathcal{L})^{2j+1}\boldsymbol{X}_n + \sum_{j=0}^{\infty}\frac{t^{2j+1}}{(2j+1)!}(\mathcal{D}i\mathcal{L})^{2j+2}\boldsymbol{X}_n = \begin{pmatrix} -[H_s\tilde{\boldsymbol{A}}\cdot(\tilde{\boldsymbol{c}}(t)\cdot\boldsymbol{p} + \tilde{\boldsymbol{d}}(t)\cdot\delta\boldsymbol{r})]_n \\ [\tilde{\boldsymbol{M}}^{-1}\cdot(\tilde{\boldsymbol{a}}(t)\cdot\boldsymbol{p} + \tilde{\boldsymbol{b}}(t)\cdot\delta\boldsymbol{r})]_n \end{pmatrix}, \tag{B20}$$

where $\tilde{\boldsymbol{a}}(t) := \cos(t\tilde{\boldsymbol{g}})$, $\tilde{\boldsymbol{b}}(t) := -\sin(t\tilde{\boldsymbol{g}})\cdot\tilde{\boldsymbol{g}}^{-1}\cdot H_s\tilde{\boldsymbol{A}}$, $\tilde{\boldsymbol{c}}(t) := \sin(t\tilde{\boldsymbol{g}}^\dagger)\cdot(\tilde{\boldsymbol{g}}^\dagger)^{-1}\cdot\tilde{\boldsymbol{M}}^{-1}$, and $\tilde{\boldsymbol{d}}(t) := \cos(t\tilde{\boldsymbol{g}}^\dagger)$ are $\nu\times\nu$ matrices. [Note that $\tilde{\boldsymbol{g}}^{-1}$ itself does not exist but $\sin(t\tilde{\boldsymbol{g}})\cdot\tilde{\boldsymbol{g}}^{-1}$ in $\tilde{\boldsymbol{b}}(t)$ does. The same goes for $(\tilde{\boldsymbol{g}}^\dagger)^{-1}$ in $\tilde{\boldsymbol{c}}(t)$.] The orthogonal condition $\langle\boldsymbol{F}(t),\boldsymbol{X}_n\rangle = 0$ is satisfied. Introducing the quantities

$$\tilde{\boldsymbol{p}}(t) := \tilde{\boldsymbol{a}}(t)\cdot\boldsymbol{p} + \tilde{\boldsymbol{b}}(t)\cdot\delta\boldsymbol{r}, \tag{B21}$$

$$\delta\tilde{\boldsymbol{r}}(t) := \tilde{\boldsymbol{c}}(t)\cdot\boldsymbol{p} + \tilde{\boldsymbol{d}}(t)\cdot\delta\boldsymbol{r}, \tag{B22}$$

Eq. (B20) is rewritten as

$$\boldsymbol{F}(t) = \begin{pmatrix} -[H_s\tilde{\boldsymbol{A}}\cdot\delta\tilde{\boldsymbol{r}}(t)]_n \\ [\tilde{\boldsymbol{M}}^{-1}\cdot\tilde{\boldsymbol{p}}(t)]_n \end{pmatrix} =: \begin{pmatrix} f_B(t) \\ v_B(t) \end{pmatrix}, \tag{B23}$$

where $f_B(t)$ is the random force on the tagged bead, and $v_B = 0$ because the (n,n) element of $\tilde{\boldsymbol{M}}^{-1}$ is 0.

Note that the only difference between the actual force $d\boldsymbol{X}_n(t)/dt = (f(t),v(t))$ of Eq. (B7) and the random force $\boldsymbol{F}(t) = (f_B(t),v_B(t))$ is that $\boldsymbol{A}$ and $\boldsymbol{M}^{-1}$ in the former are $\tilde{\boldsymbol{A}}$ and $\tilde{\boldsymbol{M}}^{-1}$ in the latter, respectively. Relevant information on the tagged bead [the (n,n) element of $\boldsymbol{A}$ and $\boldsymbol{M}^{-1}$] in the random force is subtracted and appears as the frequency matrix defined by Eq. (A6):

$$i\boldsymbol{\Omega} = \langle\dot{\boldsymbol{X}}_n,\boldsymbol{X}_n\rangle\cdot\langle\boldsymbol{X}_n,\boldsymbol{X}_n\rangle^{-1} = \begin{pmatrix} 0 & -k_BT\big/\langle\delta r_n^2\rangle_{eq} \\ k_BT\big/\langle p_n^2\rangle_{eq} & 0 \end{pmatrix} = \begin{pmatrix} 0 & -H_s/C_{nn} \\ 1/m & 0 \end{pmatrix}. \tag{B24}$$

The fluctuation-dissipation theorem is shown to hold between the memory-function matrix $\boldsymbol{\gamma}(t)$ in Eq. (B8) and the autocorrelation function of the random force $\boldsymbol{F}(t)$ in the $(p_n,\delta r_n)$ space [see Eq. (A8)]:

$$\boldsymbol{\gamma}(t) = \langle\boldsymbol{F}(t),\boldsymbol{F}\rangle\cdot\langle\boldsymbol{X}_n,\boldsymbol{X}_n\rangle^{-1} = \begin{pmatrix} \zeta(t)/m & 0 \\ 0 & 0 \end{pmatrix}, \tag{B25}$$

where

$$\zeta(t) = H_s[\tilde{\boldsymbol{a}}(t)\cdot\tilde{\boldsymbol{A}}]_{nn}. \tag{B26}$$

A matrix $\tilde{\boldsymbol{g}}$ in $\tilde{\boldsymbol{a}}(t) = \cos(t\tilde{\boldsymbol{g}})$ can be written as $\tilde{\boldsymbol{g}} = \sqrt{\boldsymbol{A}_0}\omega_\mu/2$ where ω_μ is given by Eq. (5) and $\boldsymbol{A}_0$ is a modified Rouse matrix all of whose elements in the nth column are reset to 0, i.e., when $\nu = 5$ and $n = 3$ for example,

$$\boldsymbol{A}_0 := \begin{pmatrix} 1 & -1 & 0 & 0 & 0 \\ -1 & 2 & 0 & 0 & 0 \\ 0 & -1 & 0 & -1 & 0 \\ 0 & 0 & 0 & 2 & -1 \\ 0 & 0 & 0 & -1 & 1 \end{pmatrix}. \tag{B27}$$

All elements in the nth column of $\tilde{\boldsymbol{a}}(t) = \cos(\sqrt{\boldsymbol{A}_0}\omega_\mu t/2)$ are also 0, and therefore the nth column of a matrix multiplied from the right side of $\tilde{\boldsymbol{a}}(t)$ does not affect the product. Since $\tilde{\boldsymbol{A}}$ is equivalent to $\boldsymbol{A}$ except for the (n,n) element, both give the same result when $\tilde{\boldsymbol{a}}(t)$ is multiplied from the right side by these matrices. Therefore, Eq. (B26) can be expressed as Eq. (4).

APPENDIX C: DERIVATION OF Eq. (12)

Here we derive the GLE (12) of a tracer bead in a three-dimensional isotropic viscoelastic solid. A tracer bead is characterized by a six-dimensional vector $\boldsymbol{X}_\mathrm{b} := (\boldsymbol{p}_\mathrm{b}, \delta\boldsymbol{r}_\mathrm{b})$ where $\delta\boldsymbol{r}_\mathrm{b} = \boldsymbol{r}_\mathrm{b} - \bar{\boldsymbol{r}}_\mathrm{b}$ is the displacement of the bead from its mean position $\bar{\boldsymbol{r}}_\mathrm{b}$. According to the projection-operator method (see Appendix A), the equation of motion for $\boldsymbol{X}_\mathrm{b}(t)$ is written in the form of a GLE as

$$\frac{d\boldsymbol{X}_\mathrm{b}(t)}{dt} = i\boldsymbol{\Omega}\cdot\boldsymbol{X}_\mathrm{b}(t) - \int_0^t \boldsymbol{\gamma}(t-t')\cdot\boldsymbol{X}_\mathrm{b}(t')dt' + \boldsymbol{F}(t). \tag{C1}$$

The random force $\boldsymbol{F}(t)$ in the $(\boldsymbol{p}_\mathrm{b}, \delta\boldsymbol{r}_\mathrm{b})$ space has only its $\boldsymbol{p}_\mathrm{b}$ component, i.e. [see Eq. (A7)],

$$\boldsymbol{F}(t) = e^{t\mathcal{D}i\mathcal{L}}\mathcal{D}i\mathcal{L}\boldsymbol{X}_\mathrm{b} = \begin{pmatrix} \boldsymbol{f}_\mathrm{B}(t) \\ \boldsymbol{0} \end{pmatrix}. \tag{C2}$$

According to the fluctuation-dissipation theorem [see Eq. (A8)], the memory-function matrix in the $(\boldsymbol{p}_\mathrm{b}, \delta\boldsymbol{r}_\mathrm{b})$ space reduces to

$$\boldsymbol{\gamma}(t) = \langle \boldsymbol{F}(t), \boldsymbol{F}\rangle \cdot \langle \boldsymbol{X}_\mathrm{b}, \boldsymbol{X}_\mathrm{b}\rangle^{-1} = \begin{pmatrix} \delta\zeta(t)/m & \boldsymbol{0} \\ \boldsymbol{0} & \boldsymbol{0} \end{pmatrix}, \tag{C3}$$

where the memory function $\zeta(t)$ is related to the random force $f_\mathrm{B}(t)$ by the fluctuation-dissipation theorem in real space,

$$\langle \boldsymbol{f}_\mathrm{B}(t)\boldsymbol{f}_\mathrm{B}(0)\rangle_\mathrm{eq} = \langle \boldsymbol{f}_\mathrm{B}(t), \boldsymbol{f}_\mathrm{B}\rangle = k_\mathrm{B}T\zeta(t)\boldsymbol{\delta}. \tag{C4}$$

The frequency matrix in the $(\boldsymbol{p}_\mathrm{b}, \delta\boldsymbol{r}_\mathrm{b})$ space is written as [see Eq. (A6)]

$$i\boldsymbol{\Omega} = \langle \dot{\boldsymbol{X}}_\mathrm{b}, \boldsymbol{X}_\mathrm{b}\rangle \cdot \langle \boldsymbol{X}_\mathrm{b}, \boldsymbol{X}_\mathrm{b}\rangle^{-1} = \begin{pmatrix} \boldsymbol{0} & -H_\mathrm{e}\boldsymbol{\delta} \\ \frac{1}{m}\boldsymbol{\delta} & \boldsymbol{0} \end{pmatrix}, \tag{C5}$$

where H_e is given by Eq. (13). Thus, by changing the lower integral limit of the memory integral from 0 to $-\infty$, the GLE for the bead displacement in real space is obtained as Eq. (12).

APPENDIX D: DERIVATION OF THE MSD OF A BEAD IN THE FOUR-PARAMETER MODEL MEDIUM

Equation (20) can be approximately divided into two parts:

$$\langle \overline{\Delta\delta r_\mathrm{b}^2}[\omega]\rangle_\mathrm{eq} \simeq \langle \overline{\Delta\delta r_\mathrm{b}^2}[\omega]\rangle_\mathrm{eq}^{(1)} + \langle \overline{\Delta\delta r_\mathrm{b}^2}[\omega]\rangle_\mathrm{eq}^{(2)}, \tag{D1}$$

where

$$\langle \overline{\Delta\delta r_\mathrm{b}^2}[\omega]\rangle_\mathrm{eq}^{(1)} := \frac{6k_\mathrm{B}T}{i\omega}\frac{\frac{\lambda H+\zeta_0}{\lambda H_\mathrm{e}+\lambda H+\zeta_0}}{(m+\lambda\zeta_0)(i\omega)^2 + (\lambda H_\mathrm{e}+\lambda H+\zeta_0)i\omega + H_\mathrm{e}} \tag{D2}$$

describes the behavior at $\omega \ll 1/\lambda$, whereas

$$\langle \overline{\Delta\delta r_\mathrm{b}^2}[\omega]\rangle_\mathrm{eq}^{(2)} := \frac{6k_\mathrm{B}T}{i\omega}\frac{\lambda}{\lambda m(i\omega)^2 + (m+\lambda\zeta_0)(i\omega) + \lambda H_\mathrm{e} + \lambda H + \zeta_0} \tag{D3}$$

represents the behavior at $\omega \gg 1/\lambda$. This approximation is rather good under the plausible condition $m \ll \lambda\zeta$ that is usually realized in actual systems [10]. Analysis of the MSD becomes easier by this separation, because the denominator becomes quadratic with respect to $i\omega$. Equation (D2) is derived by neglecting the highest-order terms of $i\omega$ in both denominator and numerator of $\langle \overline{\Delta\delta r_\mathrm{b}^2}[\omega]\rangle_\mathrm{eq}$ [Eq. (20)], and by multiplying the coefficient $\frac{\lambda H+\zeta_0}{\lambda H_\mathrm{e}+\lambda H+\zeta_0}$ to correctly reproduce the proper zero-frequency limit $\langle \overline{\Delta\delta r_\mathrm{b}^2}[\omega\to 0]\rangle_\mathrm{eq} = \frac{6k_\mathrm{B}T}{i\omega H_\mathrm{e}}$. On the other hand, Eq. (D3) is obtained by neglecting the lowest-order terms in both denominator and numerator of $\langle \Delta\delta r_\mathrm{b}^2[\omega]\rangle_\mathrm{eq}$.

Factorizing the denominator of Eq. (D2), we have

$$\langle \overline{\Delta\delta r_\mathrm{b}^2}[\omega]\rangle_\mathrm{eq}^{(1)} = \frac{6k_\mathrm{B}T}{m+\lambda\zeta_0}\frac{\frac{\lambda H+\zeta_0}{\lambda H_\mathrm{e}+\lambda H+\zeta_0}}{i\omega(i\omega+1/\tau_\mathrm{b}')(i\omega+1/\tau_\mathrm{e}')}, \tag{D4}$$

where

$$\tau_\mathrm{b,e}' := \frac{2(m+\lambda\zeta_0)}{\lambda H_\mathrm{e}+\lambda H+\zeta_0 \pm \sqrt{(\lambda H_\mathrm{e}+\lambda H+\zeta_0)^2 - 4H_\mathrm{e}(m+\lambda\zeta_0)^2}}. \tag{D5}$$

τ_b' (τ_e') takes the positive (negative) sign. Using the relation for the inverse one-sided Fourier transform (or the inverse Laplace transform)

$$\bar{\mathfrak{F}}\left\{\frac{1}{i\omega(i\omega+1/\tau_\mathrm{b}')(i\omega+1/\tau_\mathrm{e}')}\right\} = \tau_\mathrm{b}'\tau_\mathrm{e}' + \frac{1}{1/\tau_\mathrm{b}'-1/\tau_\mathrm{e}'}(\tau_\mathrm{b}'e^{-t/\tau_\mathrm{b}'} - \tau_\mathrm{e}'e^{-t/\tau_\mathrm{e}'}), \tag{D6}$$

we obtain the corresponding MSD in the time domain for $t \gg \lambda$ as

$$\langle \Delta\delta r_\mathrm{b}^2(t)\rangle_\mathrm{eq}^{(1)} = \frac{6k_\mathrm{B}T(\lambda H+\zeta_0)}{H_\mathrm{e}(\lambda H_\mathrm{e}+\lambda H+\zeta_0)}\left[1 + \frac{1}{2}\left(\frac{1}{\sqrt{1-(\lambda_\mathrm{e}'/\lambda_\mathrm{b}')^2}} - 1\right)e^{-t/\tau_\mathrm{b}'} - \frac{1}{2}\left(\frac{1}{\sqrt{1-(\lambda_\mathrm{e}'/\lambda_\mathrm{b}')^2}} + 1\right)e^{-t/\tau_\mathrm{e}'}\right], \tag{D7}$$

where

$$\lambda_\mathrm{b}' := \sqrt{\tau_\mathrm{b}'\tau_\mathrm{e}'} = \sqrt{\frac{m+\lambda\zeta_0}{H_\mathrm{e}}}, \tag{D8}$$

$$\lambda_\mathrm{e}' := \frac{2}{1/\tau_\mathrm{b}'+1/\tau_\mathrm{e}'} = \frac{2(m+\lambda\zeta_0)}{\lambda H_\mathrm{e}+\lambda H+\zeta_0}. \tag{D9}$$

Similarly, Eq. (D3) is written as

$$\left\langle \overline{\Delta\delta r_{\rm b}^2}[\omega] \right\rangle_{\rm eq}^{(2)} := \frac{6k_{\rm B}T}{m} \frac{1}{i\omega(i\omega + 1/\tau_{\rm b})(i\omega + 1/\tau_{\rm e})}, \tag{D10}$$

where $\tau_{\rm b}$ and $\tau_{\rm e}$ are given by Eq. (22). In the time domain ($t \ll \lambda$), it is written as

$$\left\langle \Delta\delta r_{\rm b}^2(t) \right\rangle_{\rm eq}^{(2)} = \frac{6k_{\rm B}T\lambda}{\lambda H_{\rm e} + \lambda H + \zeta_0} \left[1 + \frac{1}{2}\left(\frac{1}{\sqrt{1-(\lambda_{\rm e}/\lambda_{\rm b})^2}} - 1 \right) e^{-t/\tau_{\rm b}} - \frac{1}{2}\left(\frac{1}{\sqrt{1-(\lambda_{\rm e}/\lambda_{\rm b})^2}} + 1 \right) e^{-t/\tau_{\rm e}} \right], \tag{D11}$$

where

$$\lambda_{\rm b} := \sqrt{\tau_{\rm b}\tau_{\rm e}} = \sqrt{\frac{m\lambda}{\lambda H_{\rm e} + \lambda H + \zeta_0}}, \tag{D12}$$

$$\lambda_{\rm e} := \frac{2}{1/\tau_{\rm b} + 1/\tau_{\rm e}} = \frac{2m\lambda}{m + \lambda\zeta_0}. \tag{D13}$$

Under the condition that $\tau_{\rm b}$ and $\tau_{\rm e}$ have imaginary parts and therefore the MSD oscillates, it is convenient to express Eq. (D11) in terms of trigonometric functions as

$$\left\langle \Delta\delta r_{\rm b}^2(t) \right\rangle_{\rm eq}^{(2)} = \frac{6k_{\rm B}T\lambda}{\lambda H_{\rm e} + \lambda H + \zeta_0} \left[1 - e^{-t/\lambda_{\rm e}} \left(\cos\omega_m t + \frac{m + \lambda\zeta_0}{\sqrt{4m\lambda(\lambda H_{\rm e} + \lambda H + \zeta_0) - (m + \lambda\zeta_0)^2}} \sin\omega_m t \right) \right], \tag{D14}$$

where the frequency ω_m of the oscillation is given by Eq. (26).

APPENDIX E: DISPLACEMENT FIELD OF VISCOELASTIC SOLIDS

The deformation of an elastic or viscoelastic body is characterized by the displacement field $\boldsymbol{u}(\boldsymbol{r},t)$ at the position $\boldsymbol{r}$ at time t from its zero-stress position [35]. Due to incompressibility, the displacement field satisfies the condition $\nabla \cdot \boldsymbol{u}(\boldsymbol{r},t) = 0$. The momentum conservation condition leads to the equation of motion for the displacement field as

$$\rho \frac{\partial^2 \boldsymbol{u}(\boldsymbol{r},t)}{\partial t^2} = -\nabla \cdot \boldsymbol{\tau}(\boldsymbol{r},t) - \nabla p(\boldsymbol{r},t), \tag{E1}$$

where ρ is the medium density. Equation (E1) requires a constitutive equation relating the stress $\boldsymbol{\tau}$ to the displacement field. Due to the linearity in the stress-displacement relation in the limit of small strain, the expression for an incompressible, purely elastic (Hookean) solid is [35]

$$\boldsymbol{\tau}(\boldsymbol{r},t) = -G[\nabla \boldsymbol{u}(\boldsymbol{r},t) + [\nabla \boldsymbol{u}(\boldsymbol{r},t)]^\dagger], \tag{E2}$$

where G is the (static) shear modulus. For compressible solids, the pressure $p(\boldsymbol{r},t)$ is replaced by $-\lambda\nabla \cdot \boldsymbol{u}(\boldsymbol{r},t)$, where $\lambda := K - \frac{2}{3}G$ is the Lamé coefficient and K is the bulk modulus. For incompressible solids, both λ and K are infinity for a finite G, and $\nabla \cdot \boldsymbol{u}(\boldsymbol{r},t) = 0$, keeping the product of λ and $\nabla \cdot \boldsymbol{u}(\boldsymbol{r},t)$ finite [36].

On the other hand, the stress of viscoelastic solids depends on the history of the past displacement. Taking account of this memory effect, the constitutive equation for incompressible viscoelastic solids is

$$\boldsymbol{\tau}(\boldsymbol{r},t) = \int_{-\infty}^{t} \mathcal{M}(t-t')[\nabla \boldsymbol{u}(\boldsymbol{r},t') + [\nabla \boldsymbol{u}(\boldsymbol{r},t')]^\dagger]dt', \tag{E3}$$

where $\mathcal{M}(t)$ is the memory function associated with the relaxation modulus $G(t)$ in the frequency domain by $\overline{\mathcal{M}}[\omega] = -G^*(\omega)$. The time retardation of the stress to the applied deformation is the result of the viscoelasticity of the medium [20]. In the Fourier domain, the constitutive equation (E3) is expressed as

$$\boldsymbol{\tau}[\omega] = -G^*(\omega)[\nabla \boldsymbol{u}[\omega] + (\nabla \boldsymbol{u}[\omega])^\dagger] \tag{E4}$$

where the argument $\boldsymbol{r}$ of $\boldsymbol{\tau}$ and $\boldsymbol{u}$ is omitted for simplicity.

By putting Eq. (E3) into Eq. (E1), we have

$$\rho \frac{\partial^2 \boldsymbol{u}(\boldsymbol{r},t)}{\partial t^2} = -\int_{-\infty}^{t} \mathcal{M}(t-t')\nabla^2 \boldsymbol{u}(\boldsymbol{r},t')dt' - \nabla p(\boldsymbol{r},t). \tag{E5}$$

We derive the resistance force on a spherical bead embedded in the medium described by Eq. (E5) under a sticky boundary condition such that the medium adheres perfectly to the surface of the bead. We employ a system of coordinates with their origin at the instantaneous position of the bead center [26]. The boundary conditions are written as $\boldsymbol{u}(|\boldsymbol{r}| = R,t) = \delta\boldsymbol{r}_{\rm b}(t)$ at the bead surface, and $\boldsymbol{u}(|\boldsymbol{r}| = \infty,t) = 0$ at distances far away from the bead. By taking the two-sided Fourier transform, Eq. (E5) becomes in the frequency domain

$$-\rho\omega^2 \boldsymbol{u}[\omega] = G^*(\omega)\nabla^2 \boldsymbol{u}[\omega] - \nabla p[\omega]. \tag{E6}$$

Equation (E6) and the boundary conditions are equivalent to those for the velocity field $\boldsymbol{v}[\omega]$ of incompressible viscoelastic fluids (in which a bead is embedded) with creeping flow in the frequency domain [10,25] if $\boldsymbol{u}[\omega]$ is replaced by $\boldsymbol{v}[\omega]/(i\omega)$. The velocity field $\boldsymbol{v}[\omega]$ of viscoelastic fluids is the same as that for Newtonian fluids in the frequency domain except that the Newtonian viscosity is replaced by the dynamic viscosity [10], and the velocity field for the Newtonian fluids is known (see Ref. [26] for example). With the help of these results for fluids, the radial component u_r and the polar component u_θ of the displacement field in the frequency domain are obtained as shown in Sec. IV A.

[1] J. D. Ferry, *Viscoelastic Properties of Polymers*, 3rd ed. (Wiley, New York, 1980).
[2] S. Yamada, D. Wirtz, and S. C. Kuo, Biophys. J. **78**, 1736 (2000).
[3] A. Mukhopadhyay and S. Granick, Curr. Opin. Colloid Interface Sci. **6**, 423 (2001).
[4] T. A. Waigh, Rep. Prog. Phys. **68**, 685 (2005).
[5] E. M. Furst, Curr. Opin. Colloid Interface Sci. **10**, 79 (2005).
[6] Y. Kimura, J. Phys. Soc. Jpn. **78**, 041005 (2009).
[7] T. M. Squires and T. G. Mason, Annu. Rev. Fluid Mech. **42**, 413 (2010).
[8] T. G. Mason and D. A. Weitz, Phys. Rev. Lett. **74**, 1250 (1995).
[9] T. G. Mason, Rheol. Acta **39**, 371 (2000).
[10] T. Indei, J. D. Schieber, A. Córdoba, and E. Pilyugina, Phys. Rev. E **85**, 021504 (2012).
[11] B. D. Hoffman, G. Massiera, K. M. V. Citters, and J. C. Crocker, Proc. Natl. Acad. Sci. USA **103**, 10259 (2006).
[12] G. Massiera, K. M. V. Citters, P. L. Biancaniello, and J. C. Crocker, Biophys. J. **93**, 3703 (2007).
[13] S. A. McKinley, L. Yao, and M. G. Forest, J. Rheol. **53**, 1487 (2009).
[14] R. Kubo, M. Toda, and N. Hashitsume, *Statistical Physics II: Nonequilibrium Statistical Mechanics* (Springer-Verlag, Berlin, 1985).
[15] M. Grimm, S. Jeneyab, and T. Franosch, Soft Matter **7**, 2076 (2011).
[16] H. Mori, Prog. Theor. Phys. **33**, 423 (1965).
[17] J. M. Deutch and R. Silbey, Phys. Rev. A **3**, 2049 (1971).
[18] K. Wada and J. Hori, Prog. Theor. Phys. **49**, 129 (1973).
[19] K. Wada, Prog. Theor. Phys. **49**, 1130 (1973).
[20] R. B. Bird, R. C. Armstrong, and O. Hassager, *Dynamics of Polymeric Liquids Vol II: Kinetic Theory*, 2nd ed. (Addison-Wesley, New York, 1987).
[21] K. F. Graff, *Wave Motion in Elastic Solids* (Dover, New York, 1991), Chap. 1.
[22] L. D. Landau and E. M. Lifshitz, *Statistical Physics, Part 1*, 3rd ed. (Butterworth-Heinmann, London, 1980), Vol. 5.
[23] J. Fricks, L. Yao, T. C. Elston, and M. G. Forest, SIAM J. Appl. Math. **69**, 1277 (2009).
[24] A. Córdoba, T. Indei, and J. D. Schieber, J. Rheol. **56**, 185 (2012).
[25] R. Zwanzig and M. Bixon, Phys. Rev. A **2**, 2005 (1970).
[26] L. D. Landau and E. M. Lifshitz, *Fluid Mechanics*, 2nd ed. (Butterworth-Heinemann, London, 1987), Vol. 6.
[27] A. B. Basset, Philos. Trans. R. Soc., A **179**, 43 (1888).
[28] H. Lamb, *Hydrodynamics*, 6th ed. (Dover, New York, 1932).
[29] G. G. Stokes, Trans. Cambridge Philos. Soc. **9**, 8 (1856).
[30] N. Willenbacher and C. Oelschlaeger, Curr. Opin. Colloid Interface Sci. **12**, 43 (2007).
[31] T. Annable, R. Buscall, R. Ettelaie, and D. Whittlestone, J. Rheol. **37**, 695 (1993).
[32] H. Rehage and H. Hoffmann, J. Phys. Chem. **92**, 4712 (1988).
[33] T. Franosch, M. Grimm, M. Belushkin, F. M. Mor, G. Foffi, L. Forró, and S. Jeney, Nature (London) **478**, 85 (2011).
[34] Y. Roichman, B. Sun, A. Stolarski, and D. G. Grier, Phys. Rev. Lett. **101**, 128301 (2008).
[35] L. D. Landau and E. M. Lifshitz, *Theory of Elasticity*, 3rd ed. (Butterworth-Heinmann, London, 1986), Vol. 7.
[36] A. E. H. Love, *A Treatise on the Mathematical Theory of Elasticity*, 4th ed. (Dover, New York, 1944).